

Theory of one-phonon-assisted energy transfer between rare-earth ions in crystalsShangda Xia^{1,2} and Peter A. Tanner¹¹*Department of Biology and Chemistry, City University of Hong Kong, Tat Chee Avenue, Kowloon, Hong Kong, People's Republic of China*²*Structure Research Laboratory, Chinese Academy of Sciences; Department of Physics, University of Science and Technology of China, Hefei, Anhui, People's Republic of China*

(Received 29 October 2001; revised manuscript received 4 September 2002; published 19 December 2002)

A theoretical framework and the method of application are presented to describe nonresonant energy transfer processes between rare-earth ions of the f^N electronic configuration at centrosymmetric sites of crystals, in which the energy mismatch is made up by the emission or absorption of one “nondiagonal” phonon. The established theory of Holstein, Lyo, and Orbach (HLO) is applicable to, for example, an (EQ \leftrightarrow EQ,V) energy transfer process which is composed of an allowed pure electric quadrupole-electric quadrupole (EQ-EQ) nonradiative transition and a vibrational transition in which one “diagonal” phonon emission or absorption occurs from a definite electronic state of the donor or acceptor. By contrast, the theory applies to an (EQ \leftrightarrow EDV) process where an EQ transition occurs at one site and one nondiagonal phonon in an electric dipole vibronic (EDV) transition is involved at the other site. We find that for the (EQ \leftrightarrow EDV) process the coherent cancellations occurring in the conventional diagonal HLO theory of one-phonon-assisted processes, which lead to the dominance of two-phonon energy transfer processes, do not occur in the nondiagonal one-phonon-assisted case. First, the Debye phonon model used by HLO theory has been employed, in which the crystal is assumed to consist of an isotropic, continuous medium. This model is only applicable to acoustic phonons with small wave vector \mathbf{q} . The energy transfer rate obtained for the nondiagonal one-phonon-assisted process increases quadratically with increasing intersite energy mismatch, when it is small compared with the average thermal energy $k_B T$ at temperature T . Second, to take into account the crystal structure on the atomic scale which usually has anisotropic properties and to consider optical phonons, etc., the phonon involved in the diagonal and nondiagonal energy transfer process has been described by a running lattice wave, as an irreducible representation basis component of the space group and of the solution of lattice dynamical equations. The transition element and transition rate thus obtained show that the significant difference between the coherence effects of the diagonal and nondiagonal cases still occurs. Furthermore, some new points arise, especially the contributions from flat parts of the dispersion curves of optical phonon branches, to the studied processes. Therefore, contrary to the conclusion of HLO theory, optical phonons with $\mathbf{q}=0$ can make important contributions to one-phonon-assisted energy transfer processes for the nondiagonal case. In addition, the approximations inherent in the widely used spectral overlap model are pinpointed, and the selection rules and coherence effect of lattice waves are briefly discussed. Noticeably, although we focus upon centrosymmetric systems, however, the nondiagonal processes and the related results obtained in this paper are also applicable to noncentrosymmetric systems.

DOI: 10.1103/PhysRevB.66.214305

PACS number(s): 78.20.-e, 63.20.-e

I. INTRODUCTION

Rare-earth-ion(-doped) materials exhibit pseudoatomic sharp-line f^N - f^N luminescence which is parity forbidden by the electric dipole (ED) mechanism (to first order). Transitions are enabled by a (second-order) ED mechanism with the odd-parity component of the crystal field Hamiltonian H_{cf} and/or electron-phonon coupling Hamiltonian H_{ph} (with an odd-parity phonon for centrosymmetric systems) as the perturbation operator. Upconversion, quenching, and migration phenomena show that energy transfer is of major importance in the solid state. Resonant energy transfer has been treated by Dexter.¹ A (second-order) theory of phonon-assisted energy transfer in which a parity-allowed (in the first order) nonradiative electronic transition of the donor-acceptor system is followed or preceded by a “diagonal” phonon emission or absorption (from a definite electronic state of the donor or acceptor), making up the energy mismatch between the ions at two sites, was developed by Hol-

stein, Lyo, and Orbach² some decades ago. In the present work we focus on another important type of nonresonant energy transfer termed nondiagonal phonon-assisted energy transfer. For example, in the case of this nondiagonal electric quadrupole-electric dipole vibronic (EQ \leftrightarrow EDV) energy transfer process, one phonon is involved in an EDV transition at one site to make up the energy mismatch, while also introducing odd-parity electronic operators making a transition between a $4f^N$ state and a virtual $4f^{N-1}5d$ state, etc. An EQ transition occurs at the other site. In the notation employed, the hyphen separates the donor and acceptor sites, but the double-headed arrow serves to show that the process is composed of (EQ-EDV) and (EDV-EQ). To our knowledge, the nondiagonal phonon-assisted energy transfer theory has not been well developed up to the present,³ even though some experimental results remain unaccounted for.^{4,5} We anticipated, however, that nondiagonal phonon-assisted energy transfer would manifest some properties rather different from those of the diagonal process.

In the Holstein-Lyo-Orbach (HLO) theory, a cancellation occurs in the t -matrix element of one-phonon-assisted diagonal energy transfer between the corresponding terms of ground and excited states and between the donor and acceptor when the transition involves one low-momentum phonon and similar donor and acceptor ions, so that this process is unimportant. However, in this paper, we point out that this cancellation does not occur for nondiagonal processes, with the consequence that a faster energy transfer rate is expected to result.

Just as in HLO theory, first in the derivation and the discussion of the theory, we assume that the participating phonon is approximately of the Debye type. However, this is not appropriate for describing optical phonons and acoustic phonons with large wave vector, because of the implicit assumption that the crystal is a continuous, isotropic medium. For a more realistic treatment, second, the lattice wave model of vibrations, considering the crystal structure on an atomic scale and, therefore, the anisotropic properties, has been introduced and incorporated into the energy transfer theory. However, to take the localization of the rare-earth ion-phonon coupling into account and for the convenience of step-by-step approximative calculations, we have also adopted shell models of phonons to express the localized coupling Hamiltonian. Then the transition element and transition rate of both the diagonal and nondiagonal one-phonon-assisted energy transfer processes have been obtained and discussed based on the lattice wave model and shell model of phonons. The different coherence factors for the diagonal and nondiagonal processes obtained within the Debye phonon model are found to be unchanged, and an optical phonon with zero wave vector can make an important contribution to the nondiagonal one-phonon-assisted energy transfer process, in contrast to the conclusion of the HLO theory. Finally, we discuss under what approximation our results can resemble those from the usual spectral overlap approach (SOA).

In Sec. II the transition elements t_{fi} for the diagonal and nondiagonal processes are derived following the HLO theory. In Sec. III, the rare-earth ion-phonon coupling Hamiltonian H_{ph} based on the Debye model is defined and the element t_{fi} of the nondiagonal process is rewritten in terms of the first-order approximative wave functions caused by H_{ph} . Furthermore, more tractable methods of application and

estimation of the transition element and its selection rules, ensuing from application of the Judd closure approximation, are described. In Sec. IV, the energy migration rate W for the nondiagonal process is obtained based on the Debye model of phonons, and the dependence upon energy mismatch and upon temperature for several limiting cases is discussed. In Sec. V we review the shell model and the lattice wave model of phonons, and discuss their interrelationship. In Sec. VI, we give the expression of the electron-phonon coupling Hamiltonian based on the models in Sec. V. This is followed by the derivation of the elements t_{fi} of both diagonal and nondiagonal single-phonon-assisted energy transfer, the simplification of the latter, and the discussion of some selection rules about the phonon involved. Section VII provides the expressions for the energy migration rates of these processes based on Secs. V and VI. Discussions are then included of the summation over wave vector and different branches of the dispersion curves of phonons, and of the coherence factor. In addition, a discussion of the relationship between the present t -matrix approach and the SOA for the nondiagonal processes is made. Finally, the main conclusions of this study are given in Sec. VIII.

For simplicity, we assume that the rare-earth ions are located at centrosymmetric sites in the following discussion. The effects of changes in the equilibrium positions of nuclei in normal vibrations, which accompany electronic transitions, are ignored since these are minor for the case studied.⁶

II. (EQ↔EQ,V) AND (EQ↔EDV) t -MATRIX ELEMENTS

Figure 1 shows a typical energy transfer scheme from an excited donor $|1^*\rangle$ to a ground-state acceptor $|2\rangle$. As an example, only the EQ type of parity-allowed f^N-f^N transition is considered for the donor and acceptor transitions. We use the notation (EQ↔EQ,V) to represent this diagonal energy transfer, in which an electric-quadrupole–electric-quadrupole nonradiative electronic transition of the donor-acceptor system is followed or preceded by a vibrational transition which could occur either at the donor or at the acceptor site. Therefore, both (EQ-EQ,V) and (V,EQ-EQ) are included. Then, for this one-phonon-assisted energy transfer process with the intersite energy mismatch $\Delta E_{12} = E_2 - E_1 = \mp \hbar \omega_{s,\mathbf{q}}$, the expression for the t -matrix element, from conventional HLO theory, is

$$t_{fi} = \sum_{j=1,2} \langle 1,2^*,n_{s,\mathbf{q}} \pm 1 | \left[\frac{H_{QQ} |1^*,2,n_{s,\mathbf{q}} \pm 1\rangle \langle 1^*,2,n_{s,\mathbf{q}} \pm 1 | H_{\text{ph}}(j)}{[E_1 - (E_1 \pm \hbar \omega_{s,\mathbf{q}})]} + \frac{H_{\text{ph}}(j) |1,2^*,n_{s,\mathbf{q}} \pm 1\rangle \langle 1,2^*,n_{s,\mathbf{q}} | H_{QQ}}{(E_1 - E_2)} \right] |1^*,2,n_{s,\mathbf{q}}\rangle \right. \\ \left. = \frac{J \langle n_{s,\mathbf{q}} \pm 1 | \varepsilon | n_{s,\mathbf{q}} \rangle e^{\mp i\mathbf{q} \cdot \mathbf{R}_2}}{-\Delta E_{12}} \{ [f(1) - g(1)] e^{\pm i\mathbf{q} \cdot \mathbf{R}} - [f(2) - g(2)] \}. \quad (1)$$

where

$$J = \langle 1,2^* | H_{QQ} | 1^*,2 \rangle \quad (2)$$

and

$$\langle j, n_{s,\mathbf{q}} \pm 1 | H_{\text{ph}}(j) | j, n_{s,\mathbf{q}} \rangle = \langle n_{s,\mathbf{q}} \pm 1 | \varepsilon | n_{s,\mathbf{q}} \rangle e^{\mp i\mathbf{q} \cdot \mathbf{R}_j} f(j), \quad (3a)$$

for the ground electronic state $|j\rangle$,

$$\langle j^*, n_{s,\mathbf{q}} \pm 1 | H_{\text{ph}}(j) | j^*, n_{s,\mathbf{q}} \rangle = \langle n_{s,\mathbf{q}} \pm 1 | \varepsilon | n_{s,\mathbf{q}} \rangle e^{\mp i\mathbf{q} \cdot \mathbf{R}_j} g(j), \quad (3b)$$

for the excited electronic state $|j^*\rangle$,

s and \mathbf{q} denote the polarization and wave vector of the phonon involved, respectively, and $\mathbf{R} = \mathbf{R}_2 - \mathbf{R}_1$.

It is straightforward to observe that the cancellation arises from the opposite sign in front of the term $[g(1)e^{\mp i\mathbf{q} \cdot \mathbf{R}_1} + f(2)e^{\mp i\mathbf{q} \cdot \mathbf{R}_2}]$ and the term $[f(1)e^{\mp i\mathbf{q} \cdot \mathbf{R}_1} + g(2)e^{\mp i\mathbf{q} \cdot \mathbf{R}_2}]$. The energy denominator of the former term $\mp \hbar \omega_{s,\mathbf{q}}$, representing the phonon emission or absorption before energy transfer, is exactly opposite to that in the latter, $E_1 - E_2$, representing phonon emission or absorption after energy transfer. It is evident from Eq. (1) that the opposite sign leads to (i) the cancellation between $f(j)$ and $g(j)$, and (ii) if $\mathbf{q} \cdot \mathbf{R} \ll 1$ and ion 1 is similar to ion 2, the cancellation between the donor and acceptor will be fairly complete. This makes the single-phonon-assisted energy transfer process unimportant, so that higher-order processes need to be considered.

However, if the electronic transition of the donor or acceptor is parity forbidden, as, for example, in the $f^N - f^N$ ED transition of a rare-earth ion, another kind of single-phonon-assisted energy transfer process plays an important role, which exhibits very different characteristics. In this process,

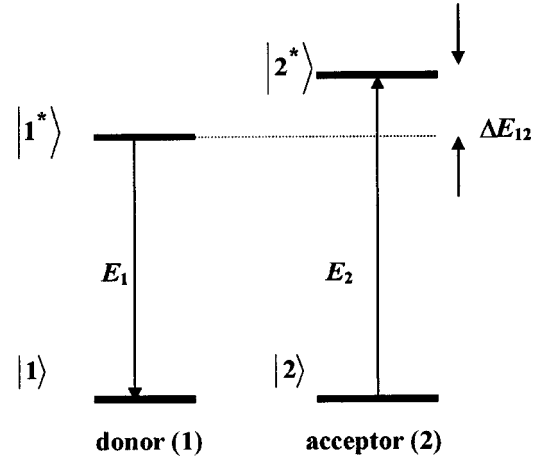


FIG. 1. Scheme for diagonal phonon-assisted energy transfer from donor (1) to acceptor (2). $\Delta E_{12} = E_2 - E_1 = \hbar \omega_{s,\mathbf{q}}$ is the intersite energy mismatch, being >0 for phonon absorption.

only an odd-parity phonon is involved in a nonradiative EDV transition at the donor or acceptor ion. Following the formalism of the HLO theory, the t -matrix element of the (EQ \leftrightarrow EDV) process is

$$t_{fi} = \langle 1, 2^*, n_{s,\mathbf{q}} \pm 1 | \left\{ \sum_{2_x} \left[\frac{H_{QD} | 1^*, 2_x, n_{s,\mathbf{q}} \pm 1 \rangle \langle 1^*, 2_x, n_{s,\mathbf{q}} \pm 1 | H_{\text{ph}}(2) + \frac{H_{\text{ph}}(2) | 1, 2_x, n_{s,\mathbf{q}} \rangle \langle 1, 2_x, n_{s,\mathbf{q}} | H_{QD}}{(E_1 - E_2)} \right] \right. \\ \left. + \sum_{1_x} \left[\frac{H_{DQ} | 1_x, 2, n_{s,\mathbf{q}} \pm 1 \rangle \langle 1_x, 2, n_{s,\mathbf{q}} \pm 1 | H_{\text{ph}}(1) + \frac{H_{\text{ph}}(1) | 1_x, 2^*, n_{s,\mathbf{q}} \rangle \langle 1_x, 2^*, n_{s,\mathbf{q}} | H_{DQ}}{(E_1 - E_{1_x} - E_2)} \right] \right\} | 1^*, 2, n_{s,\mathbf{q}} \rangle, \quad (4)$$

$$\equiv \left\{ \sum_{1_x} \left[\frac{J_{1,1_x} g_{1_x,1^*} + f_{1,1_x} J_{1_x,1^*}}{-E_{1_x}} \right] e^{\mp i\mathbf{q} \cdot \mathbf{R}_1} + \sum_{2_x} \left[\frac{J_{2^*,2_x} f_{2_x,2^*} + g_{2^*,2_x} J_{2_x,2^*}}{-E_{2_x}} \right] e^{\mp i\mathbf{q} \cdot \mathbf{R}_2} \right\} \langle n_{s,\mathbf{q}} \pm 1 | \varepsilon | n_{s,\mathbf{q}} \rangle, \quad (5)$$

$$= \langle n_{s,\mathbf{q}} \pm 1 | \varepsilon | n_{s,\mathbf{q}} \rangle e^{\mp i\mathbf{q} \cdot \mathbf{R}_2} \left[\sum_{1_x} \frac{J_{1,1_x} g_{1_x,1^*} + f_{1,1_x} J_{1_x,1^*}}{-E_{1_x}} e^{\pm i\mathbf{q} \cdot \mathbf{R}_1} + \sum_{2_x} \frac{J_{2^*,2_x} f_{2_x,2^*} + g_{2^*,2_x} J_{2_x,2^*}}{-E_{2_x}} \right], \quad (6)$$

where the electronic transition matrix elements include EQ-allowed transitions:

$$J_{1,1_x} = \langle 1, 2^* | H_{DQ} | 1_x, 2 \rangle \quad \text{and} \quad (7a)$$

$$J_{1_x,1^*} = \langle 1_x, 2^* | H_{DQ} | 1^*, 2 \rangle \supset 2^* \leftarrow 2,$$

$$J_{2^*,2_x} = \langle 1, 2^* | H_{QD} | 1^*, 2_x \rangle \quad \text{and} \quad (7b)$$

$$J_{2_x,2^*} = \langle 1, 2_x | H_{QD} | 1^*, 2 \rangle \supset 1 \leftarrow 1^*,$$

and the nondiagonal vibronic transition matrix elements of H_{ph} are given by:

$$\langle 1_x, n_{s,\mathbf{q}} \pm 1 | H_{\text{ph}}(1) | 1^*, n_{s,\mathbf{q}} \rangle \\ = \langle n_{s,\mathbf{q}} \pm 1 | \varepsilon | n_{s,\mathbf{q}} \rangle g_{1_x,1^*} e^{\mp i\mathbf{q} \cdot \mathbf{R}_1}, \\ \langle 1, n_{s,\mathbf{q}} \pm 1 | H_{\text{ph}}(1) | 1_x, n_{s,\mathbf{q}} \rangle = \langle n_{s,\mathbf{q}} \pm 1 | \varepsilon | n_{s,\mathbf{q}} \rangle f_{1,1_x} e^{\mp i\mathbf{q} \cdot \mathbf{R}_1}, \\ \langle 2_x, n_{s,\mathbf{q}} \pm 1 | H_{\text{ph}}(2) | 2, n_{s,\mathbf{q}} \rangle = \langle n_{s,\mathbf{q}} \pm 1 | \varepsilon | n_{s,\mathbf{q}} \rangle f_{2_x,2} e^{\mp i\mathbf{q} \cdot \mathbf{R}_2}, \\ \langle 2^*, n_{s,\mathbf{q}} \pm 1 | H_{\text{ph}}(2) | 2_x, n_{s,\mathbf{q}} \rangle \\ = \langle n_{s,\mathbf{q}} \pm 1 | \varepsilon | n_{s,\mathbf{q}} \rangle g_{2^*,2_x} e^{\mp i\mathbf{q} \cdot \mathbf{R}_1}. \quad (8)$$

Using this notation, in formula (3) the coefficients $g(j) = g_{j^*,j^*}$ and $f(j) = f_{j,j}$ are diagonal elements.

In the derivation from Eq. (4) to Eq. (5), the approximations

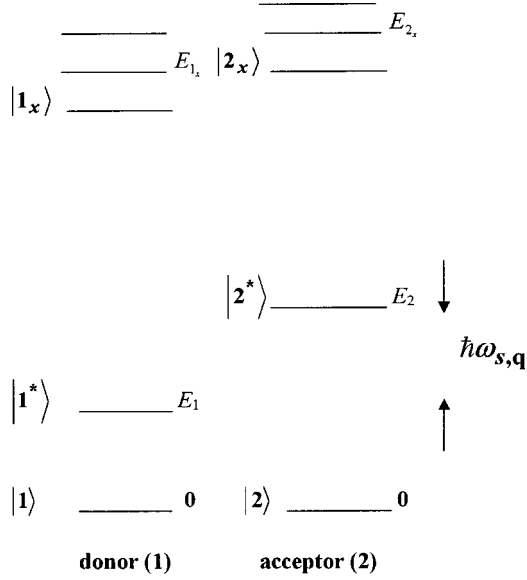


FIG. 2. Representation scheme for nondiagonal phonon-assisted energy transfer from donor (1) to acceptor (2). The phonon energy $\hbar\omega_{s,q}$ is equal to the intersite energy mismatch.

$$-E_{2_x} \mp \hbar\omega_{s,q} \approx E_1 - E_{2_x} \approx -E_{2_x} \ll 0, \quad (9a)$$

$$(E_1 - E_{1_x}) \mp \hbar\omega_{s,q} \approx E_1 - E_2 - E_{1_x} \approx -E_{1_x} \ll 0, \quad (9b)$$

have been employed. Since the energies E_{1_x} , E_{2_x} are energies within the configuration $(4f^{N-1})(5d)^1$, then $|-E_{i_x}|$ is much bigger than the phonon energies $\hbar\omega_{s,q}$, E_1 and E_2 , as shown in Fig. 2. As mentioned before, the cancellation in the diagonal (EQ \leftrightarrow EQ, V) transition element [see Eq. (1)] arises from the opposite sign in front of the two terms contained in it, which is due to the energy of the intermediate state being one phonon higher or lower than that of the initial state. However, due to the relationship (9), the two terms corresponding to the different operating order of H_{QD} and $H_{ph}(2)$ in Eq. (4) have almost the same denominators, with these being dominated by the same energy with the same sign ($-E_{2_x}$). This is also the case for the two terms related to H_{DQ} and $H_{ph}(1)$. Therefore, the above cancellations (i) and (ii) occurring in the diagonal (EQ \leftrightarrow EQ, V) process *do not* occur in the nondiagonal (EDV \leftrightarrow EQ) process.

III. ELECTRON-PHONON COUPLING HAMILTONIAN AND ONE-PHONON-ASSISTED ENERGY TRANSFER MATRIX ELEMENT BASED UPON THE DEBYE PHONON MODEL

We have presented a description of the Debye model of vibration and the localized electron-phonon coupling within this model in Appendix A.

If we introduce the direction averaged strain tensor $\varepsilon(\mathbf{R}_j)$ at \mathbf{R}_j , then we may write the localized electron-phonon coupling Hamiltonian as

$$H_{ph}(j) = \frac{\partial H_{cf}(\mathbf{R}_j)}{\partial \varepsilon(\mathbf{R}_j)} \varepsilon(\mathbf{R}_j), \quad (10)$$

so that the matrix element:

$$\begin{aligned} & \langle j^*, n_{s,q} \pm 1 | H_{ph}(j) | j^*, n_{s,q} \rangle \\ &= \langle j^* | \frac{\partial H_{cf}(\mathbf{R}_j)}{\partial \varepsilon(\mathbf{R}_j)} | j^* \rangle \langle n_{s,q} \pm 1 | \varepsilon(\mathbf{R}_j) | n_{s,q} \rangle \quad (11) \\ &= g(j) \langle n_{s,q} \pm 1 | \varepsilon | n_{s,q} \rangle e^{\mp i\mathbf{q} \cdot \mathbf{R}_j}, \quad (12) \end{aligned}$$

where, as in HLO theory, we introduce the coefficient $g(j)$. Utilizing the expression (A11) of $\varepsilon(\mathbf{R}_j)$ and the matrix element (A12) of ε from the HLO treatment,² from Eqs. (11) and (12) we obtain the following expression for $g(j)$ used in the HLO theory as follows:

$$g(j) = \langle j^* | \frac{\partial H_{cf}(\mathbf{R}_j)}{\partial \varepsilon(\mathbf{R}_j)} | j^* \rangle. \quad (13)$$

Similarly,

$$f(j) = \langle j | \frac{\partial H_{cf}(\mathbf{R}_j)}{\partial \varepsilon(\mathbf{R}_j)} | j \rangle. \quad (14)$$

If we use Eqs. (A13) and (A14), we may obtain more detailed expressions (A16) and (A17) for $g(j)$ and $f(j)$, respectively, in which only the terms with even k contribute.

Now it is possible to write the coupling parameters in Eqs. (6) and (8) for the nondiagonal (EQ \leftrightarrow EDV) energy transfer process as follows:

$$g_{1_x, 1^*} = \langle 1_x | \frac{\partial H_{cf}(\mathbf{R}_1)}{\partial \varepsilon(\mathbf{R}_1)} | 1^* \rangle, \quad (15)$$

and so on. By the crystal field expansion of the H_{cf} , as in Eq. (A13), we have the expressions (A19) and (A20), etc., in which only the terms with odd t contribute.

Moreover, if we use the perturbation theory taking $H_{ph}(j)$ as the perturbation Hamiltonian, we may make the transition t -matrix elements (4)–(6) simpler and physically clearer. For example, we may have the following first-order approximate initial and terminal states:

$$\begin{aligned} |[1^*], 2, n_{s,q}\rangle &= |1^*, 2, n_{s,q}\rangle + \sum_{1_x} |1_x, 2, n_{s,q} \pm 1\rangle \\ &\times \frac{\langle 1_x, 2, n_{s,q} \pm 1 | H_{ph}(1) | 1^*, 2, n_{s,q}\rangle}{E_1 - (E_{1_x} \pm \hbar\omega_{s,q})}, \quad (16) \end{aligned}$$

$$\begin{aligned} \langle [1], 2^*, n_{s,q} \pm 1 | &= \langle 1, 2^*, n_{s,q} \pm 1 | + \sum_{1_x} \langle 1_x, 2^*, n_{s,q} | \\ &\times \frac{\langle 1, 2^*, n_{s,q} \pm 1 | H_{ph}(1) | 1_x, 2^*, n_{s,q}\rangle}{\pm \hbar\omega_{s,q} - E_{1_x}}. \quad (17) \end{aligned}$$

The $H_{ph}(2)$ can also give similar states. By referring to Eqs. (7), (11), (12) and (A19), (A20), etc., we see the t -matrix element (4)–(6) can be rewritten as

$$t_{fi} \equiv \langle [1], 2^*, n_{s,q} \pm 1 | H_{DQ} | [1^*], 2, n_{s,q} \rangle + \langle 1, [2^*], n_{s,q} \pm 1 | H_{DQ} | 1^*, [2], n_{s,q} \rangle \quad (18)$$

$$= \langle n_{s,q} \pm 1 | \varepsilon | n_{s,q} \rangle e^{\mp i \mathbf{q} \cdot \mathbf{R}_2} [\langle [1], 2^* | H_{DQ} | [1^*], 2 \rangle e^{\pm i \mathbf{q} \cdot \mathbf{R}} + \langle 1, [2^*] | H_{DQ} | 1^*, [2] \rangle], \quad (19)$$

where

$$\langle [1], 2^* | H_{DQ} | [1^*], 2 \rangle \equiv \sum_{1_x} \frac{J_{1,1_x} g_{1_x,1^*} + f_{1,1_x} J_{1_x,1^*}}{-E_{1_x}}, \quad (20)$$

$$\langle 1, [2^*] | H_{DQ} | 1^*, [2] \rangle \equiv \sum_{2_x} \frac{J_{2^*,2_x} f_{2_x,2} + g_{2^*,2_x} J_{2_x,2}}{-E_{2_x}}, \quad (21)$$

in which $|[1^*]\rangle$ is the first-order approximative wave function of the donor, corrected by $\partial H_{cf}(\mathbf{R}_1)/\partial \varepsilon(\mathbf{R}_1)$ in Eq. (10) of $H_{ph}(1)$.

To make the electronic transition matrix element in Eq. (20) more tractable, first we write the ED-EQ interaction Hamiltonian between the donor and acceptor as a spherical tensor:^{7,8}

$$H_{DQ} = \frac{e^2}{R^4} \sum_{q_1 q_2} C_{q_1 q_2}^{12}(\Theta, \Phi) D_{q_1}^{(1)}(D) D_{q_2}^{(2)}(A), \quad (22)$$

where

$$C_{q_1 q_2}^{12}(\Theta, \Phi) = -\sqrt{\frac{7!}{2!4!}} \begin{pmatrix} 1 & 2 & 3 \\ q_1 & q_2 & -(q_1+q_2) \end{pmatrix} \times C_{q_1+q_2}^{(3)}(\Theta, \Phi)^*, \quad (23)$$

in which Θ and Φ belong to the polar coordinates (R, Θ, Φ) of vector \mathbf{R} and

$$C_q^{(k)} = \sqrt{\frac{4\pi}{2k+1}} Y_q^{(k)}. \quad (24)$$

Then we use the well-known Judd closure approximation for the matrix element:⁹

$$\begin{aligned} & \langle [1], 2^* | H_{DQ} | [1^*], 2 \rangle \\ &= \frac{e^2}{R^4} \sum_{q_1 q_2} C_{q_1 q_2}^{12}(\Theta, \Phi) \langle 2^* | D_{q_2}^{(2)} | 2 \rangle \langle [1] | D_{q_1}^{(1)} | [1^*] \rangle, \\ &\equiv \frac{e^2}{R^4} \sum_{q_1 q_2} C_{q_1 q_2}^{12}(\Theta, \Phi) \langle 2^* | D_{q_2}^{(2)} | 2 \rangle \sum_{\lambda t p} \langle 1 | U_{p+q_1}^{(\lambda)} | 1^* \rangle \\ &\quad \times (-1)^{p+q} [\lambda] \begin{pmatrix} 1 & \lambda & t \\ q_1 & -(p+q_1) & p \end{pmatrix} A_{tp}^\lambda(\varepsilon), \quad (25) \end{aligned}$$

where

$$A_{tp}^\lambda(\varepsilon) = \frac{\partial A_p^t(\mathbf{R}_1)}{\partial \varepsilon(\mathbf{R}_1)} \Xi(t, \lambda), \quad (26)$$

in which the expression for $\Xi(t, \lambda)$ was given by Judd.⁹ The values of the parameters $A_{tp}^\lambda(\varepsilon)$ can be obtained by fitting the corresponding EDV transition intensities in the absorption or emission spectra, based upon the model used herein, in which the phonons are described by the Debye model.

From Eq. (25) it is evident that for (EDV \leftrightarrow EQ) energy transfer, the EDV transition (of the donor, say) satisfies the same selection rules for total angular momentum J as does an ED transition of a rare-earth ion in a noncentrosymmetric system. That is, the triangle relation (J_f, λ, J_i) with $\lambda = 2, 4, 6$ must be satisfied. Furthermore, the EQ transition (of the acceptor, say) has selection rules based upon $(J_f, 2, J_i)$.

IV. (EDV \leftrightarrow EQ) ENERGY TRANSFER RATE BASED UPON THE DEBYE MODEL

Following the HLO model we take the donor and acceptor ions to be identical and $f(1) \approx f(2) = f$, $g(1) \approx g(2) = g$, which means that $|1^*\rangle$ is similar to $|2^*\rangle$, as is the case for energy migration. Then using the Fermi golden rule together with Eq. (6) we obtain the (EDV \leftrightarrow EQ) energy transfer rate

$$W_{2 \leftarrow 1} = \frac{2\pi}{\hbar} \sum_{s,q} |t_{fi}|^2 \delta(\hbar \omega_{s,q} \pm \Delta E_{12}), \quad (27)$$

$$\begin{aligned} & \equiv \frac{2\pi}{\hbar} |\langle [1], 2^* | H_{DQ} | [1^*], 2 \rangle|^2 \\ & \times \sum_{s,q} [|\langle n_{s,q} \pm 1 | \varepsilon | n_{s,q} \rangle|^2 \\ & \times h_N^I(\mathbf{q}, \mathbf{R}) \delta(\hbar \omega_{s,q} \pm \Delta E_{12})], \quad (28) \end{aligned}$$

where

$$\begin{aligned} |\langle [1], 2^* | H_{DQ} | [1^*], 2 \rangle|^2 &= \left| \sum_{1_x} \frac{J_{1,1_x} g_{1_x,1^*} + f_{1,1_x} J_{1_x,1^*}}{-E_{1_x}} \right|^2 \\ &= \left| \sum_{2_x} \frac{J_{2^*,2_x} f_{2_x,2} + g_{2^*,2_x} J_{2_x,2}}{-E_{2_x}} \right|^2 \\ &= |\langle 1, [2^*] | H_{DQ} | 1^*, [2] \rangle|^2 \quad (29) \end{aligned}$$

and

$$h_N^I(\mathbf{q}, \mathbf{R}) = |e^{\pm i \mathbf{q} \cdot \mathbf{R}} + 1|^2. \quad (30)$$

Note that the HLO coherence factor for the diagonal process is given by a formula similar to Eq. (30), but with a negative instead of positive sign, in Ref. 2. In the derivation of Eqs. (28) and (29) we have used the following relations:

$$J_{2_x,2} = J_{1,1_x}^*, \quad g_{2^*,2_x} = g_{1_x,1^*}^*, \quad (31)$$

$$J_{2^*,2_x} = J_{1_x,1^*}^*, \quad f_{2_x,2} = f_{1,1_x}^*, \quad (32)$$

$$\begin{aligned} J_{1,1_x} g_{1_x,1^*} &= \langle 1, 2^* | H_{DQ} | 1_x, 2 \rangle \langle 1_x, 2 | \frac{\partial H_{cf}(\mathbf{R}_1)}{\partial \varepsilon(\mathbf{R}_1)} | 1^*, 2 \rangle \\ &= (J_{1,1_x} g_{1_x,1^*})^*. \quad (33) \end{aligned}$$

The quantities on the left-hand side of Eq. (33) are real, since $|1^*,2\rangle$ and $|1,2^*\rangle$ have the same phase factor, and $\langle 1_x,2|\langle 1_x,2|$ is real.

The golden rule equation (28) may be evaluated under the Debye approximation. We follow the same equation (2.15) as in Ref. 2:

$$\sum_{s,\mathbf{q}} F(s,\mathbf{q}) = \frac{V}{2\pi^2} \sum_s \frac{1}{V_s^3} \int_0^{\omega_{s,D}} \langle F(s,\mathbf{q}) \rangle_{\Omega} \omega^2 d\omega,$$

for any function of s and \mathbf{q} , where V is the sample volume; $\omega = |\mathbf{q}|V_s = qV_s$ where V_s and $\omega_{s,D}$ are the spread velocity and Debye frequency for the s th polarization mode, respectively. We then obtain the energy transfer rate

$$\begin{aligned} W_{2\leftarrow 1} &= \frac{2\pi}{\hbar} |\langle [1],2^* | H_{DQ} | [1^*],2 \rangle|^2 \frac{V}{2\pi^2} \sum_s \frac{1}{V_s^5} \left[\frac{\alpha_s |\Delta E_{12}|^3}{2NM} \right] \\ &\times \left\{ \frac{n(|\Delta E_{12}|) + 1}{n(|\Delta E_{12}|)} \right\} \langle h_N^I(\mathbf{q},\mathbf{R}) \rangle_{\Omega} \frac{1}{\hbar^3} \\ &= \frac{|\Delta E_{12}|^3}{2\pi\hbar^4\rho} |\langle [1],2^* | H_{DQ} | [1^*],2 \rangle|^2 \\ &\times \sum_s \frac{\alpha_s}{V_s^5} \left\{ \frac{n(|\Delta E_{12}|) + 1}{n(|\Delta E_{12}|)} \right\} \langle h_N^I(\mathbf{q},\mathbf{R}) \rangle_{\Omega}, \end{aligned} \quad (34)$$

where ρ is the mass density, and $n(|\Delta E_{12}|) = [e^{(|\Delta E_{12}|)/k_B T} - 1]^{-1}$. We conclude that the energy transfer rate is observed to be proportional to $|\Delta E_{12}|^3$, which differs from the linear dependence upon $|\Delta E_{12}|$ in the HLO diagonal energy transfer model.

We now analyze Eq. (34) under the two limits of energy mismatches. In the case of the energy mismatch between the two sites being large (of the order of 100 cm^{-1}), the wavelength of the phonon involved in nonresonant energy transfer is of the same order as the intersite separation, $\mathbf{q} \cdot \mathbf{R} \gg 1$. The coherence factor averages out:

$$\langle h_N^I(\mathbf{q},\mathbf{R}) \rangle_{\Omega} = \langle 2[1 + \cos \mathbf{q} \cdot \mathbf{R}] \rangle_{\Omega} = 2 \left(1 + \frac{\sin qR}{qR} \right) \approx 2, \quad (35)$$

and we obtain a simple expression for the transfer rate,

$$\begin{aligned} W_{2\leftarrow 1} &= \frac{|\Delta E_{12}|^3}{\pi\hbar^4\rho} |\langle [1],2^* | H_{DQ} | [1^*],2 \rangle|^2 \\ &\times \sum_s \frac{\alpha_s}{V_s^5} \left\{ \frac{n(|\Delta E_{12}|) + 1}{n(|\Delta E_{12}|)} \right\}, \end{aligned} \quad (36)$$

for the emission or absorption of a phonon of energy ΔE_{12} .

It is not difficult to obtain the vibronic transition rate $W_{2^*\leftarrow 2}$ of EDV absorption for the acceptor ion within the Debye phonon model as follows:

$$W_{2^*\leftarrow 2} = \frac{(\Delta E)^3}{2\pi\hbar^4\rho} |\langle [2^*] | H_{ED} | [2] \rangle|^2 \sum_s \frac{\alpha_s}{V_s^5} [n(\Delta E) + 1], \quad (37)$$

where the photon-electronic excitation energy difference $\Delta E = \hbar\omega_{\gamma} - E_2$ is equal to the energy $\hbar\omega$ of the phonon created. It is evident that the dependences of $W_{2\leftarrow 1}$ upon $|\Delta E_{12}|$ and $n(|\Delta E_{12}|)$ are the same [concerning the matrix element, refer to the relation between the far left side and the far right side of Eq. (29)] as those of $W_{2^*\leftarrow 2}$ in Eq. (37), since $\langle h_N^I(\mathbf{q},\mathbf{R}) \rangle_{\Omega} \approx 2$ is independent of \mathbf{q} , and both Eqs. (36) and (37) are based on the density of states $\rho_s(\omega) = V\omega^2/2\pi^2V_s^3 \propto \omega^2 \propto \Delta E^2$ of the Debye phonons.

We now consider further two limiting cases: when

$$|\Delta E_{12}|/k_B T \ll 1:$$

$$W_{2\leftarrow 1} \approx \frac{(\Delta E_{12})^2}{\pi\hbar^4\rho} |\langle [1],2^* | H_{DQ} | [1^*],2 \rangle|^2 \sum_s \frac{\alpha_s}{V_s^5} (k_B T) \quad (38)$$

and when

$$|\Delta E_{12}|/k_B T \gg 1:$$

$$\begin{aligned} W_{2\leftarrow 1} &\approx \frac{(|\Delta E_{12}|)^3}{\pi\hbar^4\rho} |\langle [1],2^* | H_{DQ} | [1^*],2 \rangle|^2 \\ &\times \sum_s \frac{\alpha_s}{V_s^5} [e^{-|\Delta E_{12}|/k_B T}]. \end{aligned} \quad (39)$$

The result (38) differs from that for the analogous diagonal one-phonon-assisted energy transfer process where the energy transfer rate is *independent* of energy mismatch. In the present case, a quadratic dependence is obtained. In both cases, however, the energy transfer rate is linearly dependent upon temperature.

Considering the case when the energy mismatch between the two sites is small, then the quantity $\mathbf{q} \cdot \mathbf{R} \ll 1$. Under this condition, the coherence factor

$$\begin{aligned} \langle h_N^I(\mathbf{q},\mathbf{R}) \rangle_{\Omega} &= 2 \left(1 + \frac{\sin qR}{qR} \right) \approx 2 \left[1 + \left(1 - \frac{1}{6} q^2 R^2 \right) \right] \\ &= 4 - \frac{1}{3} q^2 R^2 \approx 4, \end{aligned} \quad (40)$$

which is much greater than the corresponding value $2[1 - (1 - \frac{1}{6} q^2 R^2)] = \frac{1}{3} q^2 R^2$ for the diagonal process in Ref. 2. Then, we obtain for the two limiting cases:

$$|\Delta E_{12}|/k_B T \ll 1:$$

$$W_{2\leftarrow 1} \approx \frac{2(\Delta E_{12})^2}{\pi\hbar^4\rho} |\langle [1],2^* | H_{DQ} | [1^*],2 \rangle|^2 \sum_s \frac{\alpha_s}{V_s^5} (k_B T), \quad (41)$$

$$|\Delta E_{12}|/k_B T \gg 1:$$

$$\begin{aligned} W_{2\leftarrow 1} &\approx \frac{2(\Delta E_{12})^3}{\pi\hbar^4\rho} |\langle [1],2^* | H_{DQ} | [1^*],2 \rangle|^2 \\ &\times \sum_s \frac{\alpha_s}{V_s^5} [e^{-|\Delta E_{12}|/k_B T}]. \end{aligned} \quad (42)$$

For diagonal one-phonon-assisted processes, the energy transfer rate for a small energy mismatch is much smaller [by the factor $\frac{1}{3}q^2R^2:2=(qR)^2/6=(\Delta E_{12}R/V_s\hbar)^2/6$] than that for a large energy mismatch, and the process has been considered to be unimportant.² The result for the nondiagonal one-phonon-assisted process for a small energy mismatch in Eq. (41) is, however, twice of that for a large energy mismatch, in Eq. (38). This means that a small energy mismatch in nonresonant energy transfer could be made up by nondiagonal acoustic phonon processes (as long as the density of phonon states with energy $\hbar\omega_{s\mathbf{q}}=|\Delta E_{12}|$ is not too small) and that the energy transfer rate $W_{2\leftarrow 1}$ increases with increasing mismatch $|\Delta E_{12}|$. At room temperature, this mismatch may then range up to ca. 30 cm^{-1} . This is significant for energy transfer and, moreover, for energy migration, since an exact energy match between the two sites is seldom achieved. Thus the nondiagonal process is expected to be an important contributor to the energy migration and transfer mechanism in many systems. Notice that, as pointed above, the above $|\Delta E_{12}|^2$ dependence of the rate $W_{2\leftarrow 1}$ in Eqs. (38) and (41) is brought about from the same background: the Debye relation $\omega_{s\mathbf{q}}=V_sq$, as is also the rate of $W_{2\leftarrow 2}$ in Eq. (37) when $|\Delta E|\ll k_B T$. We find some experimental references (e.g., Figs. 2 and 3 in Ref. 6, Fig. 2 in Ref. 10, and Fig. 1 in Ref. 11) concerning intraconfigurational f^N-f^N transitions of rare-earth ions where the profile of lower-energy vibronic structure approximates to the density of states of the vibrations of the undisturbed lattice, i.e., is proportional to $|\Delta E|^2$, as expected from Eq. (37) under the condition that $|\Delta E|\ll k_B T$. Notice that the Debye model which we have employed is applicable to acoustic phonons, especially for phonons with small wave vector \mathbf{q} . The $|\Delta E_{12}|^2$ dependence of $W_{2\leftarrow 1}$ could only be valid within small $|\Delta E_{12}|$, which should be rather smaller than $\hbar\omega_{s,D}$.

V. LOCAL SYMMETRY SHELL MODEL AND LATTICE WAVE MODEL OF VIBRATION

Several decades ago, some studies of the vibronic transitions in the electronic spectra of rare-earth ions in solids employed lattice waves in constructing standing waves describing the local vibrations of rare-earth ion systems.¹⁰⁻¹⁴ The recent trend in this subject area, however, has been to use directly (without involving lattice waves) a moiety-mode model for the treatment of rare-earth vibrations,¹⁵⁻¹⁷ not only because of its simplicity, but also because the rare-earth ion-phonon coupling interaction is localized. In the case of energy transfer phenomena, there are two localized electron-phonon couplings involved: for the donor and acceptor ions located at rather close positions. These are coupled to each other so that many ions in the crystal are subject to both electron-phonon coupling interactions. Thus coherence effects of the running waves of the vibration need to be considered, just as in HLO theory, due to the propagation of the lattice wave between the two sites. The localized moiety model of vibrations is unable to handle these types of physical effects. Notably, for nondiagonal phonon-assisted (EQ \leftrightarrow EDV) energy transfer processes, only odd-parity phonons (in centrosymmetric systems) are involved, and the

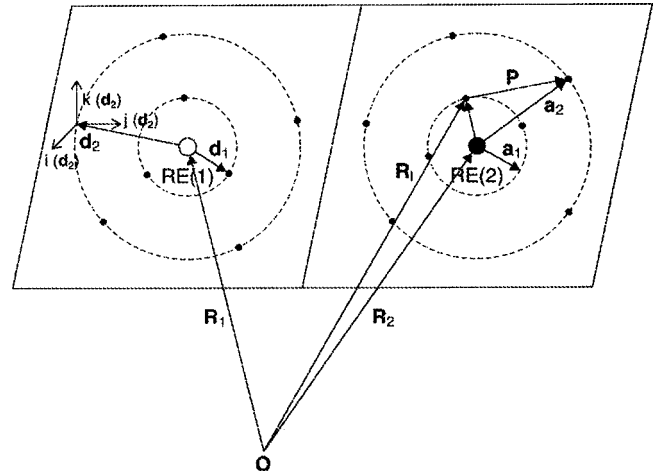


FIG. 3. Rare-earth ions and their environment of shells of atoms in a crystal. The adjacent rare-earth ions are represented by open and solid circles, and the neighboring shells of atoms by circled dots.

most important interaction is the one between the $t=1$ electric dipole of the rare-earth ion and the odd-parity phonon (say, t_{1u} in O_h symmetry) at the rare-earth site.^{10,16} The field of the electric dipole is extensive^{6,10} compared with that of an electric quadrupole ($t=2$), which is the most important field involved in the above diagonal, for example (EQ \leftrightarrow EQ, V), energy transfer process. Thus it is required to adopt the lattice wave model especially for the phonon involved in the nondiagonal phonon-assisted energy transfer process. However, in order to take into account the localization of the coupling and for the convenience of step-by-step approximate calculations, we have also adopted a site-symmetry shell model of vibrations to express the localized coupling Hamiltonian. This model follows the model calculation of the vibronic sidebands of Cs_2UBr_6 ,^{10,18} where each of the structured features in a vibronic sideband was characterized by a localized site symmetry and composed of contributions from related standing waves which are linear combinations of lattice waves. Therefore, we introduce the definitions of the localized shell model and the lattice wave model of phonons, and discuss their interrelationship.

We begin this section with the discussion of the local site-symmetry coordinate of vibration. For the convenience of considering and computing the electron-phonon coupling energy, crystal vibrations are classified according to the irreducible representations (irreps) of the site group \mathcal{G} of the rare-earth ion donor (1) and/or acceptor (2). Then the surrounding atoms are classified as shells (composed of atoms of the same type) located at the same distance $|\mathbf{d}_n|$ (or $|\mathbf{a}_n|$) from rare-earth ion 1 (or 2): see Fig. 3. For simplicity, we use the vector notation \mathbf{d}_n [or \mathbf{a}_n] itself to identify the atom located at the position $(\mathbf{R}_1 + \mathbf{d}_n)$ [or $(\mathbf{R}_2 + \mathbf{a}_n)$] and write its displacement $\mathbf{u}(\mathbf{d}_n)$ from this equilibrium position as

$$\begin{aligned} \mathbf{u}(\mathbf{d}_n) &= \sum_{\alpha} u_{\alpha}(\mathbf{d}_n) \mathbf{i}_{\alpha}(\mathbf{d}_n) \\ &= u_x(\mathbf{d}_n) \mathbf{i}(\mathbf{d}_n) + u_y(\mathbf{d}_n) \mathbf{j}(\mathbf{d}_n) + u_z(\mathbf{d}_n) \mathbf{k}(\mathbf{d}_n), \quad (43) \end{aligned}$$

where the starting point of $\mathbf{i}_\alpha(\mathbf{d}_n)$ ($\mathbf{i}_1=\mathbf{i}, \mathbf{i}_2=\mathbf{j}, \mathbf{i}_3=\mathbf{k}$), depends upon \mathbf{d}_n , but its direction is independent of \mathbf{d}_n . Then, using the projection operators of group \mathcal{G} , we can obtain the symmetry-adapted vibrational coordinate $Q^{n\beta}(D)$ of the n th shell of the rare-earth ion 1:

$$Q^{n\beta}(D) = \sqrt{M_n} u^{n\beta} = \sum_{\mathbf{d}_n, \alpha} a_\alpha^{n\beta}(\mathbf{d}_n)^* \sqrt{M_n} u_\alpha(\mathbf{d}_n), \quad (44)$$

with a similar expression for ion 2. In this equation $\sqrt{M_n} u_\alpha(\mathbf{d}_n)$ is a mass-weighted displacement coordinate of atom \mathbf{d}_n ; the index β is

$$\beta = (ith, \Gamma, \gamma) \text{ of group } \mathcal{G}, \quad (45)$$

and is a shorthand symbol for the i th ($\Gamma\gamma$) irrep of group \mathcal{G} amongst the a_Γ irreps ($\Gamma\gamma$) contained in the vibrations of the n th shell, and the transformation matrix is orthogonal (real unity) as shown in Eqs. (B1) and (B2). For example, for an octahedrally coordinated rare-earth ion, the vibrations of the six ligands contribute two symmetry-adapted t_{1u} -type $Q^{n\beta}$ moiety modes according to Eq. (44), but the *actual* two t_{1u} -type moiety-mode vibrations Q_β^n are a mixture of these modes, where the mixing coefficients are decided by the force constants of the studied system from the solutions of the appropriate dynamic equations.

We now turn our attention to the lattice wave formalism. In the following, we only utilize the symmetry-adapted $Q^{n\beta}$ to study electron-phonon coupling, whereas for the treatment of phonons themselves, we use lattice waves with normal coordinates Q_q^s , which are solutions of dynamic equations having a definite wave vector \mathbf{q} :

$$Q_q^s = \frac{1}{\sqrt{N}} \sum_{\mathbf{R}_l, \mathbf{p}, \alpha} e^{-i\mathbf{q} \cdot \mathbf{R}_l} a_\alpha^{qs}(\mathbf{p})^* \sqrt{M_p} u_\alpha(\mathbf{R}_l, \mathbf{p}), \quad (46)$$

where N =number of cells=number of \mathbf{q} in the Brillouin zone; $\sqrt{M_p} u_\alpha(\mathbf{R}_l, \mathbf{p})$ is the mass-weighted displacement coordinate of atom \mathbf{p} located at the $(\mathbf{R}_l + \mathbf{p})$ position, in which \mathbf{R}_l is the representative position of the l th primitive unit cell and the \mathbf{p} itself is used to identify the atom shifted by \mathbf{p} from the position \mathbf{R}_l . The index s is a shorthand symbol, analogous to Eq. (45):

$$s = (ith, \Gamma, \gamma) \text{ of group } \mathcal{S}(\mathbf{q}), \quad (47)$$

where the space group $\mathcal{S}(\mathbf{q})$ (a subgroup of the space group \mathcal{S} describing all the symmetry properties of the crystal) is the group of the wave vector \mathbf{q} . The actual Q_q^s are also mixtures of several symmetry-adapted coordinates $Q_{s\mathbf{q}}$ of the same type, and $Q_{s\mathbf{q}}$ can be obtained using the projection operators of group $\mathcal{S}(\mathbf{q})$.

The transformation matrix thus obtained is complex unitary as shown in Eqs. (B4) and (B5). By referring to Appendix B 2, we may have, from Eq. (46),

$$\sqrt{M_p} u_\alpha(\mathbf{R}_l, \mathbf{p}) = \frac{1}{\sqrt{N}} \sum_{\mathbf{q}, s} e^{i\mathbf{q} \cdot \mathbf{R}_l} a_\alpha^{qs}(\mathbf{p}) Q_q^s, \quad (48)$$

which means that the atom \mathbf{p} within a cell participates in the vibration of all $3\gamma N$ lattice waves, each with a definite \mathbf{q} and s (γ =number of atoms within a cell). The components of the polarization vector of atom \mathbf{p} for the lattice wave \mathbf{q}_s are $(N^{-1/2})a_\alpha^{qs}(\mathbf{p})$ multiplied by a phase factor $e^{i\mathbf{q} \cdot \mathbf{R}_l}$ determined by the particular cell the atom is located in. Equation (48) corresponds to the Eq. (A1) in the Debye model, but with complex conjugate phase factor due to use of the convention of Eq. (5) in Ref. 11.

By referring to Appendix B 3, we have

$$Q^{n\beta}(D) = \sum_{\mathbf{q}_s} \langle n\beta | \mathbf{q}_s \rangle_D Q_{\mathbf{q}_s}^s, \quad (49)$$

where

$$\langle n\beta | \mathbf{q}_s \rangle_D = \frac{1}{\sqrt{N}} \sum_{\mathbf{d}_n, \alpha} a_\alpha^{n\beta}(\mathbf{d}_n)^* a_\alpha^{qs}[\mathbf{p}(\mathbf{d}_n)] e^{i\mathbf{q} \cdot \mathbf{R}_l(\mathbf{d}_n)} \quad (50)$$

transforms the normal coordinates Q_q^s into the symmetry-adapted coordinates $Q^{n\beta}(D)$ of the n th shell around the donor ion. We note that $\langle n\beta | \mathbf{q}_s \rangle$ was introduced as $\langle \beta n | \mathbf{k}\lambda \rangle$ by Chodos and Satten,¹⁰ but without the definition in Eq. (50). Notice that the factor $N^{-1/2}$ in Eq. (50) makes the quantity $\langle n\beta | \mathbf{q}_s \rangle_D$ very small, whereas the term number $3\gamma N$ of the summation over \mathbf{q} and s in Eq. (49) is very large. Thus for any *actual* calculation, the value of N must be large enough, for example, 1012 independent \mathbf{q} in irreducible 1/48 of the Brillouin zone, which corresponds to 5154 \mathbf{q} , by extending to all wings of the \mathbf{q} star $\{\mathbf{q}\}$, each of them has a \mathbf{q} in the irreducible zone as a wing, as executed by Ref. 10.

Analogous to Eq. (50), we have for the acceptor ion

$$\langle n\beta | \mathbf{q}_s \rangle_A = \frac{1}{\sqrt{N}} \sum_{\mathbf{a}_n, \alpha} a_\alpha^{n\beta}(\mathbf{a}_n)^* a_\alpha^{qs}[\mathbf{p}(\mathbf{a}_n)] e^{i\mathbf{q} \cdot \mathbf{R}_l(\mathbf{a}_n)}. \quad (51)$$

If ion 1 is identical to ion 2 and their sites are also equivalent, we have

$$\mathbf{p}(\mathbf{a}_n) = \mathbf{p}(\mathbf{d}_n), \quad \mathbf{R}_l(\mathbf{a}_n) = \mathbf{R}_l(\mathbf{d}_n) + \mathbf{R}, \quad (52)$$

for the case $\mathbf{d}_n = \mathbf{a}_n$, so that we obtain an important relation for energy migration:

$$\langle \eta\beta | \mathbf{q}_s \rangle_A = \langle n\beta | \mathbf{q}_s \rangle_D e^{i\mathbf{q} \cdot \mathbf{R}} \quad (53)$$

VI. ELECTRON-PHONON COUPLING HAMILTONIAN AND ONE-PHONON-ASSISTED ENERGY TRANSFER MATRIX ELEMENT BASED UPON THE LATTICE WAVE MODEL OF PHONONS

Since the electron-phonon interaction is rather localized, we may expand the electron-phonon coupling Hamiltonian $H_{\text{ph}}(j)$ as

$$H_{\text{ph}}(1) = \sum_{n\beta} f_{n\beta}(D) Q^{n\beta}(D). \quad (54)$$

Substituting Eq. (49) into Eq. (54), we obtain

$$H_{\text{ph}}(1) = \sum_{n\beta} f_{n\beta}(D) \sum_{q_s} \langle n\beta | \mathbf{q}s \rangle_D Q_{\mathbf{q}}^s. \quad (55)$$

Due to the well-known relation (A7), Eq. (55) shows that $H_{\text{ph}}(1)$ contains phonon operators $Q_{\mathbf{q}}^s$ of all lattice waves via local site-symmetry displacement coordinates $Q^{n\beta}$ related to them. The effective value of n_{max} may not be large since the operator $H_{\text{ph}}(1)$ is localized (all the contributions from shells with $n > n_{\text{max}}$ can be ignored). Thus the adoption of the shell-vibration model introduces the ability to perform the step-by-step calculation of $H_{\text{ph}}(1)$.

We now consider the application of above results to the theory of one-phonon assisted energy transfer. We consider both the diagonal energy transfer case, following the formalism of HLO,² and the nondiagonal case developed above.

A. Diagonal energy transfer process

From Eqs. (55) and (A7) we have

$$\begin{aligned} & \langle 1, n_{s\mathbf{q}} \pm 1 | H_{\text{ph}}(1) | 1, n_{s\mathbf{q}} \rangle \\ &= \sum_{n,\beta} f^{n\beta}(1) \langle n\beta | \pm \mathbf{q}s \rangle_D \sqrt{\frac{\hbar}{2\omega_{s\mathbf{q}}}} \left\{ \frac{\sqrt{n_{s\mathbf{q}}+1}}{\sqrt{n_{s\mathbf{q}}}} \right\}, \end{aligned} \quad (56)$$

where

$$f^{n\beta}(1) = \langle 1 | f_{n\beta}(D) | 1 \rangle, \quad (57)$$

which can be calculated directly by Eq. (C1), or by Eqs. (C2) and (C5), and the selection rule of point group \mathcal{G} is directly applicable. Similar to Eq. (57), we may introduce $g^{n\beta}(1)$, $f^{n\beta}(2)$, and $g^{n\beta}(2)$, corresponding to $g(1)$, $f(2)$, and $g(2)$, respectively, of HLO theory.²

Therefore, by referring to Eqs. (1)–(3), the (EQ \leftrightarrow EQ, V) energy transfer matrix element is

$$\begin{aligned} t_{fi} &= \frac{J}{-\Delta E_{12}} \left\{ \frac{\sqrt{n_{s\mathbf{q}}+1}}{\sqrt{n_{s\mathbf{q}}}} \right\} \sqrt{\frac{\hbar}{2\omega_{s\mathbf{q}}}} \sum_{n,\beta} \{ \langle n\beta | \pm \mathbf{q}s \rangle_D \\ & \times [f^{n\beta}(1) - g^{n\beta}(1)] - \langle n\beta | \pm \mathbf{q}s \rangle_A [f^{n\beta}(2) - g^{n\beta}(2)] \}. \end{aligned} \quad (58)$$

Introducing Eq. (53) for migration, we obtain

$$\begin{aligned} t_{fi} &= \frac{J}{-\Delta E_{12}} \left\{ \frac{\sqrt{n_{s\mathbf{q}}+1}}{\sqrt{n_{s\mathbf{q}}}} \right\} \sqrt{\frac{\hbar}{2\omega_{s\mathbf{q}}}} \sum_{n,\beta} \langle n\beta | \pm \mathbf{q}s \rangle_A \\ & \times \{ [f^{n\beta}(1) - g^{n\beta}(1)] e^{\mp i\mathbf{q}\cdot\mathbf{R}} - [f^{n\beta}(2) - g^{n\beta}(2)] \} \end{aligned} \quad (59)$$

so that we observe that the cancellation between the two terms within the second set of curly parentheses still occurs, just as the case of HLO theory. Furthermore,

$$\begin{aligned} t_{fi} &= \frac{J}{-\Delta E_{12}} \left\{ \frac{\sqrt{n_{s\mathbf{q}}+1}}{\sqrt{n_{s\mathbf{q}}}} \right\} \sqrt{\frac{\hbar}{2\omega_{s\mathbf{q}}}} \\ & \times \left\{ \sum_{n,\beta} \langle n\beta | \pm \mathbf{q}s \rangle_A (f^{n\beta} - g^{n\beta}) \right\} (e^{\mp i\mathbf{q}\cdot\mathbf{R}} - 1), \end{aligned} \quad (60)$$

where

$$f^{n\beta} = f^{n\beta}(1) = f^{n\beta}(2), \quad g^{n\beta} = g^{n\beta}(1) = g^{n\beta}(2). \quad (61)$$

B. Nondiagonal energy transfer process

From Eqs. (55) and (A7) we have

$$\begin{aligned} & \langle 1_x, n_{s\mathbf{q}} \pm 1 | H_{\text{ph}}(1) | 1^*, n_{s\mathbf{q}} \rangle \\ &= \sum_{n,\beta} g_{1_x, 1^*}^{n\beta} \langle n\beta | \pm \mathbf{q}s \rangle_D \sqrt{\frac{\hbar}{2\omega_{s\mathbf{q}}}} \left\{ \frac{\sqrt{n_{s\mathbf{q}}+1}}{\sqrt{n_{s\mathbf{q}}}} \right\}, \end{aligned} \quad (62)$$

where

$$g_{1_x, 1^*}^{n\beta} = \langle 1_x | f_{n\beta}(D) | 1^* \rangle = \sum_{\text{odd } p} \frac{\partial A_p^t(D)}{\partial Q^{n\beta}(D)} \langle 1_x | D_p^t(D) | 1^* \rangle. \quad (63)$$

Similarly, we have analogous expressions for the electron-phonon coupling coefficients $f_{1,1_x}^{n\beta}$, $f_{2,2_x}^{n\beta}$, and $g_{2^*,2_x}^{n\beta}$. Thus, just as from the Eqs. (4)–(9), we obtain the expression of the transition matrix element for the (EQ \leftrightarrow EDV) energy transfer involving a (s, \mathbf{q}) phonon:

$$\begin{aligned} t_{fi} &= \left\{ \frac{\sqrt{n_{s\mathbf{q}}+1}}{\sqrt{n_{s\mathbf{q}}}} \right\} \sqrt{\frac{\hbar}{2\omega_{s\mathbf{q}}}} \sum_{n,\beta} \left\{ \langle n\beta | \pm \mathbf{q}s \rangle_D \right. \\ & \times \sum_{1_x} \left[\frac{J_{1,1_x} g_{1_x, 1^*}^{n\beta} + f_{1,1_x}^{n\beta} J_{1_x, 1^*}}{-E_{1_x}} \right] \\ & \left. + \langle n\beta | \pm \mathbf{q}s \rangle_A \sum_{2_x} \left[\frac{J_{2^*,2_x} f_{2_x, 2}^{n\beta} + g_{2^*,2_x}^{n\beta} J_{2_x, 2}}{-E_{2_x}} \right] \right\}. \end{aligned} \quad (64)$$

With the inclusion of Eq. (53) we obtain

$$\begin{aligned} t_{fi} &= \left\{ \frac{\sqrt{n_{s\mathbf{q}}+1}}{\sqrt{n_{s\mathbf{q}}}} \right\} \sqrt{\frac{\hbar}{2\omega_{s\mathbf{q}}}} \sum_{n,\beta} \langle n\beta | \pm \mathbf{q}s \rangle_A \\ & \times \left\{ \sum_{1_x} \left[\frac{J_{1,1_x} g_{1_x, 1^*}^{n\beta} + f_{1,1_x}^{n\beta} J_{1_x, 1^*}}{-E_{1_x}} \right] e^{\mp i\mathbf{q}\cdot\mathbf{R}} \right. \\ & \left. + \sum_{2_x} \left[\frac{J_{2^*,2_x} f_{2_x, 2}^{n\beta} + g_{2^*,2_x}^{n\beta} J_{2_x, 2}}{-E_{2_x}} \right] \right\}. \end{aligned} \quad (65)$$

It is important to observe that both of the signs inside the second curly parentheses are the same, so that the cancellation which occurs in the diagonal process is not present. Furthermore, for the case of energy migration, by using a similar discussion as in Eqs. (16)–(21) and (31)–(33), we obtain

$$t_{fi} = \left\{ \frac{\sqrt{n_{s\mathbf{q}}+1}}{\sqrt{n_{s\mathbf{q}}}} \right\} \sqrt{\frac{\hbar}{2\omega_{s\mathbf{q}}}} \sum_{n,\beta} \{ \langle n\beta | \pm \mathbf{q}s \rangle_A \} \\ \times \langle [1]_{n\beta,2^*} | H_{DQ} | [1^*]_{n\beta,2} \rangle (e^{\mp i\mathbf{q}\cdot\mathbf{R}} + 1), \quad (66)$$

where

$$\langle [1]_{n\beta,2^*} | H_{DQ} | [1^*]_{n\beta,2} \rangle = \sum_{1_x} \left[\frac{J_{1,1_x} g_{1_x,1^*}^{n\beta} + f_{1,1_x}^{n\beta} J_{1_x,1^*}}{-E_{1_x}} \right] \\ = \sum_{2_x} \left[\frac{J_{2^*,2_x} f_{2_x,2}^{n\beta} + g_{2^*,2_x}^{n\beta} J_{2_x,2}}{-E_{2_x}} \right] \\ = \langle 1, [2^*]_{n\beta} | H_{DQ} | 1^*, [2]_{n\beta} \rangle, \quad (67)$$

in which the $|[1^*]_{n\beta}\rangle$ is the first-order approximative wave function of the initial state of the donor, corrected by the coupling function $f_{n\beta}(D)$ of $H_{\text{ph}}(1)$ in Eq. (54), which is written as Eq. (C1). The two elements in Eq. (67) can also be approximately worked out by using Judd closure, as, for example, we have

$$\langle [1]_{n\beta,2^*} | H_{DQ} | [1^*]_{n\beta,2} \rangle \\ = \sum_{1_x} \left[\frac{J_{1,1_x} g_{1_x,1^*}^{n\beta} + f_{1,1_x}^{n\beta} J_{1_x,1^*}}{-E_{1_x}} \right] \\ = \frac{e^2}{R^4} \sum_{q_1 q_2} C_{q_1 q_2}^{12}(\Theta, \Phi) \\ \times \langle 2^* | D_{q_2}^{(2)} | 2 \rangle \left[\sum_{\lambda t p} \langle 1 | U_{p+q_1}^{(\lambda)} | 1^* \rangle (-1)^{p+q_1} (2\lambda+1) \right. \\ \left. \times \begin{pmatrix} 1 & \lambda & t \\ q_1 & -(p+q_1) & p \end{pmatrix} \Xi(t, \lambda) \frac{\partial A_p^t(D)}{\partial Q^{n\beta}(D)} \right], \quad (68)$$

in which

$$A_{tp}^\lambda [Q^{n\beta}(D)] = \Xi(t, \lambda) \frac{\partial A_p^t(D)}{\partial Q^{n\beta}(D)} \quad (69)$$

are considered as parameters, whose values can be obtained from the fitting of the EDV sideband intensities of transitions between the crystal field states of the donor, using the localized phonon model for $Q^{n\beta}$.¹⁷ For example, in the simplest case, under the $n_{\text{max}}=1$ approximation, a moiety mode Q^β is a linear combination of $a_{1\beta}$ shell modes, $Q^{1\beta}$. If a rare-earth ion is at an octahedral site, the most important terms in Eqs. (54) and (C1) of $H_{\text{ph}}(1)$ are those with $t=1$, which correspond to phonons $Q^{1\beta}$ with β transforming as the t_{1u} irreducible representation of the O_h point group. Thus only the two t_{1u} -type moiety-mode phonons $Q^{1\beta}$ have nonzero coefficients $\partial A_p^1 / \partial Q^{1\beta} \sim a_T$ and a_F in Ref. 16. Under the $n_{\text{max}}=2,3,\dots$ approximations, the shell method of Chodos and Satten^{10,18} is used for the phonon modes.

The selection rules on total angular momentum J of the relevant electronic transitions have been presented above.

We also have the usual site point group selection rule for an EDV transition: if we label the initial and final electronic crystal field levels of the donor or acceptor by the irreps Γ_i^e and Γ_f^e , respectively, it is necessary that the direct product $\Gamma_i^e \times \Gamma_f^e$ contains an irrep in common with an irrep contained in the direct product $\Gamma_f^e \times \Gamma_\beta$ for the phonon $Q^{n\beta}$ creation process, for example.

Besides, the projection coefficients $\langle n\beta | \pm \mathbf{q}s \rangle$ in Eq. (66) of t_{fi} contain selection rules, which can be obtained by a similar method to that used in Ref. 13. However, instead of starting from an entire irrep of the space group \mathcal{S} (a linear combination of whose basis components forms a standing wave), we should start from a ‘‘little irrep’’ of space group \mathcal{S} , i.e., from an irrep of the \mathbf{q} vector group $\mathcal{S}(\mathbf{q})$, a basis component of which is a running wave. That is, we should not multiply the character for a class of elements in group $\mathcal{S}(\mathbf{q})$ by the number k of wings in the \mathbf{q} star $\{\mathbf{q}\}$ when we determine its character in the site group.

VII. SINGLE-PHONON-ASSISTED ENERGY MIGRATION RATE BASED UPON THE LATTICE WAVE MODEL

We now consider the transfer rate for one-phonon-assisted energy transfer, according to the diagonal and nondiagonal processes. For simplicity, we only give the expression for the energy migration rate.

A. Diagonal energy transfer process

The energy migration rate W based upon Eq. (60) is

$$W = \sum_{s,\mathbf{q}} \frac{2\pi}{\hbar} |t_{fi}|^2 \delta(\hbar\omega_{s\mathbf{q}} \pm \Delta E_{12}) \\ = \frac{\hbar\pi J^2}{|\Delta E_{12}|^3} \left\{ \frac{n(|\Delta E_{12}|) + 1}{n(|\Delta E_{12}|)} \right\} \sum_{n'\beta'} [(f^{n\beta} - g^{n\beta}) \\ \times D_{nn'}^{\beta\beta'} (|\Delta E_{12}|) (f^{n'\beta'} - g^{n'\beta'})^*] \quad (70)$$

where $D_{nn'}^{\beta\beta'}$ is the effective projected density of phonon states:

$$D_{nn'}^{\beta\beta'} (|\Delta E_{12}|) = \sum_{s,\mathbf{q}} \langle n\beta | \pm \mathbf{q}s \rangle_A \langle \pm \mathbf{q}s | n'\beta' \rangle_A \\ \times \delta(\hbar\omega_{s\mathbf{q}} \pm \Delta E_{12}) |e^{\mp i\mathbf{q}\cdot\mathbf{R}} - 1|^2. \quad (71)$$

In this equation, the δ function and the factor $|e^{\mp i\mathbf{q}\cdot\mathbf{R}} - 1|^2$ describe the efficiency of the $(\pm \mathbf{q}s)$ lattice wave phonon in accomplishing the energy transfer from the points of view of energy conservation and coherence effects, respectively. The remaining two transformation matrices project the lattice wave into the shell vibration. Notice that the coherence factor does not occur in the analogous quantity $\rho_{nn'}^{\beta\beta'}$ used in Ref. 10 for vibronic band theory.

We digress here, in order to make some comparisons of our results for diagonal energy transfer with those from HLO theory, which is the only alternative theory of phonon-assisted energy transfer. It is evident from the above results

that the coherence factor is the same as in HLO theory, so that the same cancellation occurs in the energy transfer rate expression. The energy transfer rate W in Eq. (70) and the $D_{nn'}^{\beta\beta'}$ in Eq. (71) have contributions from all lattice waves ($\mathbf{q}s$). Since we are not dealing with isotropic, continuous media, the Debye-type dispersion relation $\omega_{s,\mathbf{q}} = \omega_s(\mathbf{q}) = v_s|\mathbf{q}|$ is only applicable to acoustic phonons with small $|\mathbf{q}|$, so that we require the entire dispersion relations $\omega_s(\mathbf{q})$ for all s and \mathbf{q} to be available to complete the summation over s and \mathbf{q} in the definition of $D_{nn'}^{\beta\beta'}$.

Without reference to the phonon dispersion curves of a specific system, we now give a general discussion of the contributions of different lattice wave phonons to the energy transfer process. Generally, the sum of the phonon modes is performed first over $\hat{\mathbf{R}}_j$, then over $|\mathbf{q}|$, and finally over s , as follows:

$$\sum_{s\mathbf{q}} () = \sum_s \left\{ \sum_{|\mathbf{q}|} \left[\sum_{\hat{\mathbf{R}}_j} () \right] \right\},$$

where for a certain \mathbf{q} , we have a \mathbf{q} star, $\{\mathbf{q}\} = \{\mathbf{q}_1, \mathbf{q}_2, \mathbf{q}_3, \dots, \mathbf{q}_k\} = \{\hat{\mathbf{R}}_1\mathbf{q}, \hat{\mathbf{R}}_2\mathbf{q}, \hat{\mathbf{R}}_3\mathbf{q}, \dots, \hat{\mathbf{R}}_k\mathbf{q}\}$. Here $\hat{\mathbf{R}}_j$ are operators of the crystallographic point group \mathcal{G}_0 , among which $\hat{\mathbf{R}}_1 = \hat{\mathbf{p}}$ can be any element of the point group $\mathcal{P}(\mathbf{q})$, all of which keep $\mathbf{q} = \hat{\mathbf{p}}\mathbf{q} = \mathbf{q}_1$ invariant or equivalent. However, $\hat{\mathbf{R}}_2$ gives another wing (or arm) $\mathbf{q}_2 = \hat{\mathbf{R}}_2\mathbf{q}$. The k wings of the \mathbf{q} star, \mathbf{q}_j , have the same absolute value $|\mathbf{q}_j| = |\hat{\mathbf{R}}_j\mathbf{q}| = |\mathbf{q}_1| = |\mathbf{q}|$ and have the same vibration frequency $\omega_{s\mathbf{q}_j} = \omega_{s\mathbf{q}} = \dots$. Note that each lattice wave $Q_{\mathbf{q}_j}^s$ is a running wave, thus being different from a standing wave which is a linear combination of the k coordinates $Q_{\mathbf{q}_j}^s$ related to a $\{\mathbf{q}\}$, used by Satten for the description of vibronic transition bands.¹³ However, since the different wings of a $\{\mathbf{q}\}$ can make up the same energy mismatch, we perform the summation over $\hat{\mathbf{R}}_j$ first. This summation, which is over the k wings of a definite \mathbf{q} star, can be compared with k times the ‘‘average over the solid angle Ω ’’ of the squared strain tensor [Eq. (2.6)] and of the coherence factor [Eq. (2.18), etc.] in HLO theory.² Notice, however, that our summation over wings is performed for the product of the coherence factor and the projection factors, and the $\{\mathbf{q}\}$ itself is \mathbf{q} direction dependent. Second, the summation over $|\mathbf{q}|$ can contribute remarkably to the rate W , for a few energy-suitable ‘‘flat’’ parts of the curve $\omega_s(\mathbf{q})$, lying in high-symmetry directions, around $\mathbf{q}=0$, or on the surface of the Brillouin zone. By contrast, in the Debye phonon model, all phonon propagation directions are equivalent and the dispersion relation is simply $\omega_s(\mathbf{q}) = v_s|\mathbf{q}|$. Finally, the summation over different branches s in Eq. (71) considers contributions from different branches of lattice waves. Our phonon modes have special symmetry properties indicated by the symbols s and \mathbf{q} , pertinent to the anisotropic properties and to the crystal structure on an atomic scale, which effects their contribution to energy transfer as shown in Eqs. (66) and (67). However, only two transverse waves and one longitudinal wave are introduced in HLO theory.

We now consider the phonon contribution from the viewpoint of the density of states, which is represented by the δ function in Eqs. (70) and (71), and remark upon the important differences from HLO theory. For example, flat optical branches, even near $\mathbf{q}=0$, have an appreciable density of states and phonon energy of up to several hundred cm^{-1} . These phonons can contribute to energy transfer processes with large energy mismatch. However, optical phonons are not considered in HLO theory: especially for phonons with small \mathbf{q} , one-phonon energy transfer processes are not important because the density of states of Debye phonons is then almost zero (as well as the almost zero coherence factor).

Detailed total density of states information is only available for metals and semiconductors. Considering this information, then generally, compared with the Debye-type phonon model used in Ref. 2, there are more phonons in the region $(0.4-0.6)\omega_{\max}$ [due to the flat parts of the curve $\omega_{\text{TA}}(\mathbf{q})$], fewer phonons in the region $(0.6-0.8)\omega_{\max}$ [no density of states modes or only slanting parts of $\omega_{\text{LA}}(\mathbf{q})$ therein], and more phonons in the region $(0.8-1.0)\omega_{\max}$ [due to many flat parts of $\omega_{\text{LO}}(\mathbf{q})$ and $\omega_{\text{TO}}(\mathbf{q})$] which occur and contribute to energy transfer. Few studies of the phonon density of states are available for insulators containing rare earth ions.^{10,19,20} The comparison of the phonon density of states data for Cs_2UBr_6 with the Debye phonon model shows that there are considerably more phonons in the regions $(0.1-0.3)\omega_{\max}$, $(0.38-0.45)\omega_{\max}$, and $(0.92-1.0)\omega_{\max}$ than in the Debye model, but fewer phonons in the region $(0.48-0.92)\omega_{\max}$.

B. Nondiagonal energy transfer process

Based upon Eq. (66), the energy transfer rate W is

$$W = \frac{\hbar \pi}{|\Delta E_{12}|} \left\{ \begin{array}{l} n(|\Delta E_{12}|) + 1 \\ n(|\Delta E_{12}|) \end{array} \right\} \\ \times \sum_{\substack{n\beta \\ n'\beta'}} [\langle [1]_{n\beta, 2^*} | H_{DQ} | [1^*]_{n\beta, 2} \rangle N_{nn'}^{\beta\beta'} (|\Delta E_{12}|) \\ \times \langle [1^*]_{n'\beta', 2} | H_{DQ} | [1]_{n'\beta', 2^*} \rangle], \quad (72)$$

where

$$N_{nn'}^{\beta\beta'} (|\Delta E_{12}|) = \sum_{s\mathbf{q}} \langle n\beta | \pm \mathbf{q}s \rangle_A \langle \pm \mathbf{q}s | n'\beta' \rangle_A \\ \times \delta(\hbar\omega_{s\mathbf{q}} \pm \Delta E_{12}) |e^{\mp i\mathbf{q}\cdot\mathbf{R}} + 1|^2 \quad (73)$$

is also an effective projected density of phonon states, which differs from $D_{nn'}^{\beta\beta'}$ only by the coherence factor, as we pointed out previously. Notice that the factor $J/|\Delta E_{12}|$ in Eq. (70) has its appropriate form $(J_{1,1x} \text{ or } J_{1,x,1^*})/(-E_{1x})$ contained in the definition of Eq. (67) for the element $\langle [1]_{n\beta, 2^*} | H_{DQ} | [1^*]_{n'\beta', 2} \rangle$, so that the factor $[J/|\Delta E_{12}|]^2$ does not appear in Eq. (72), but is present in Eq. (70).

The above discussions concerning the sum over s and \mathbf{q} in $D_{nn'}^{\beta\beta'}$ are also applicable for $N_{nn'}^{\beta\beta'}$. The summation of all phonon modes is first carried out over different wings of a \mathbf{q}

star, then over $|\mathbf{q}|$, and finally over different branches s in Eq. (73). As mentioned above, flat parts of optical phonon dispersion curves can make important contributions to the energy transfer process. We emphasize that this also applies to points near $\mathbf{q}=0$, which is different from our discussion of nondiagonal energy transfer in Sec. IV, where we employed the Debye phonon model in which the phonon density of states near $\mathbf{q}=0$ is negligible. Noticeably, in contrast to the conclusions from HLO theory, both the density of states and the coherence factor allow one optical phonon (even with $\mathbf{q}=0$) to make an important contribution to energy transfer processes, for the nondiagonal case.

Based upon the above approximation and treatment in Sec. VI the calculation of the energy transfer rate W in Eq. (72) becomes tractable if we have the solution of the lattice dynamic equations for all lattice waves \mathbf{q}_s . It is evident from Eq. (72) that the obtained value of W thus calculated may be very different from that obtained by the SOA or by only considering the contributions from moiety modes due to the \mathbf{q} -dependent coherence factor and transformation factors in Eq. (73).

At this point, it is pertinent to make a discussion about the coherence factor. First, for a lattice wave with low-symmetry \mathbf{q} , the number of wings in the $\{\mathbf{q}\}$ is large. Especially, with general \mathbf{q} (i.e., without any symmetry property), the number of wings is the maximum, which equals the number of operators in point group \mathcal{G}_0 (for example, 48 for O_h). In this case, the summation over different wings in a $\{\mathbf{q}\}$ approaches the “average over the solid angle” in HLO theory, mentioned in Sec. VII A. Then the coherence factor becomes

$$|e^{\mp i\mathbf{q}\cdot\mathbf{R}} \mp 1|^2 = 2(1 \mp \cos \mathbf{q}\cdot\mathbf{R}) \rightarrow 2 \left(1 \mp \frac{\sin qR}{qR} \right) \quad (74)$$

for diagonal [taking the negative sign in Eq. (74)] and nondiagonal (taking the positive sign) processes. In this case, if the donor-acceptor distance

$$R = |\mathbf{R}| \gg \frac{\lambda}{2\pi} = \frac{1}{q} \quad \text{i.e. } qR \gg 1, \quad (75)$$

then the coherence term

$$\left(\mp 2 \frac{\sin qR}{qR} \right) \rightarrow 0. \quad (76)$$

In other words, the two running waves are no longer coherent, and the results are close to the usual treatment in which the localized vibration model is usually employed. Therefore, from this point of view, the coherence effect is more remarkable for lattice waves with high-symmetry \mathbf{q} .

Second, if the donor-acceptor distance

$$R > (R_D + R_A), \quad (77)$$

which is the summation of the effective interaction radius of $H_{\text{ph}}(1)$ and $H_{\text{ph}}(2)$, respectively, then the overlap between the excitation (or deexcitation) regions of the lattice waves created (or destroyed) at the donor and acceptor does not exist any more. Therefore, the coherence effect between the two running waves could be ignored. In this case, we may

use localized mode models (including the moiety-mode model) to describe the relevant phonon involved. We notice that $(R_D + R_A)$ is quite large for the $t=1$ dipole-phonon (say, t_{1u}) coupling involved in the nondiagonal energy transfer process, as mentioned in Sec. V. Thus the running wave model is more suitable for the nondiagonal process than the diagonal process.

Third, if the rare-earth donor and acceptor are doped impurity ions, a lattice wave with definite \mathbf{q}_0 must be scattered by them, changing it to be an approximative lattice wave within a limited spatial domain (i.e., a superposition of lattice waves with \mathbf{q} 's distributing around the \mathbf{q}_0). In this case, if the donor-acceptor distance R is larger than the phonon coherence length L , the radius of the domain where the lattice wave (as a kind of collective description) of the host phonon is still valid, then the above coherence effect can also be ignored.

Now we turn to the discussion of another related subject. The “spectral overlap” approach has been extensively used in the interpretation of energy transfer phenomena, and usually no explanation is given as to why this approach can be extended to phonon-assisted energy transfer processes, and no attention has been paid to the difference between diagonal or nondiagonal processes.⁴ At this stage it is pertinent to add a comment concerning the relationship between the “ t -matrix element” approach described above and the SOA of Dexter¹ for energy transfer processes, which involve nondiagonal phonons. For the case of a one (emitted) phonon-assisted nondiagonal (EDV \leftrightarrow EQ) energy transfer process, similar to the discussion in Eqs. (16)–(21), the matrix element t_{fi} in Eq. (66) can be written as

$$t_{fi} = \langle [1], n_{s\mathbf{q}} + 1; 2^* | H_{DQ} | [1^*], n_{s\mathbf{q}}; 2 \rangle + \langle [1]; [2^*], n_{s\mathbf{q}} + 1 | H_{QD} | 1^*; [2], n_{s\mathbf{q}} \rangle. \quad (78)$$

Therefore, the two terms of Eq. (78) correspond to the two processes EDV-EQ and EQ-EDV, respectively, which are shown in Fig. 4.

Following Dexter,¹ we may first average $|\langle [1], n_{s\mathbf{q}} + 1; 2^* | H_{DQ} | [1^*], n_{s\mathbf{q}}; 2 \rangle|^2$, where \mathbf{R} contained in the H_{DQ} is assumed to vary its orientation continuously. Since this average has nothing to do with the structure of the wave function, so the inclusion of antiparity electronic states $|1_x\rangle$ needed for the nondiagonal process, and of phonon states $|n_{s\mathbf{q}} + 1\rangle$, etc., needed for phonon assistance, do not change the result shown in Eq. (21) of Ref. 1. Second, we sum $|\langle [1], n_{s\mathbf{q}} + 1; 2^* | H_{DQ} | [1^*], n_{s\mathbf{q}}; 2 \rangle|^2$ over all electronic states of the donor and acceptor, while taking $n_{s\mathbf{q}}$ as its average value $\bar{n}_{s\mathbf{q}} = (e^{\hbar\omega_{s\mathbf{q}}/k_B T} - 1)^{-1}$ at temperature T . Thus we obtain a result similar to Dexter's equation (22) (Ref. 1):

$$\begin{aligned} & |\langle [1], \overline{n_{s\mathbf{q}}} + 1; 2^* | H_{DQ} | [1^*], \overline{n_{s\mathbf{q}}}; 2 \rangle|^2 \\ & \propto |\langle [1], \overline{n_{s\mathbf{q}}} + 1 | \mathbf{r}_1 | [1^*], \overline{n_{s\mathbf{q}}} \rangle|^2 |\langle 2^* | N_2 | 2 \rangle|^2, \end{aligned} \quad (79)$$

where $\mathbf{r}_1 = \sum_i^N \mathbf{r}_{1i}$ is proportional to the electric dipole operator of the donor ion, and N_2 is the electric quadrupole operator of the acceptor ion. This expression is the basis of the

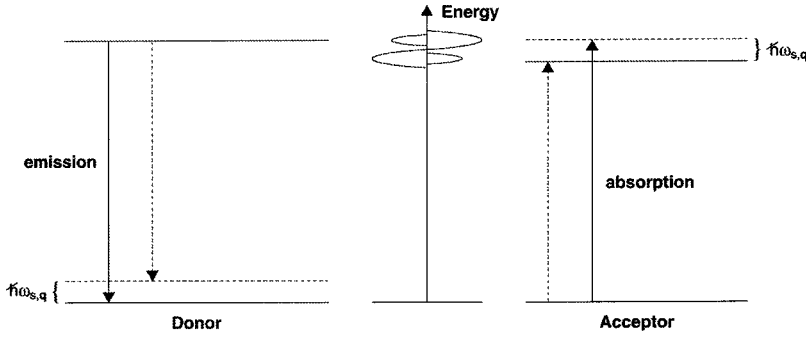


FIG. 4. Spectral overlap of rare-earth ion donor and acceptor bands. The energy scale shows the spectral overlap between the emission spectrum of the donor and the absorption spectrum of the acceptor ion. Vibronic bands are represented by broader spectral features than pure electronic transitions. Solid lines represent EQ \rightarrow EDV energy transfer, while dashed lines represent EDV \rightarrow EQ energy transfer.

SOA of calculating the EDV-EQ energy transfer rate. Similarly, the second term of Eq. (78) forms the basis of the SOA for EQ-EDV energy transfer, which for energy migration gives the same result as the SOA for EDV-EQ energy transfer, according to Eqs. (66) and (67).

However, the complex square $|t_{fi}|^2$ in Eq. (78) contains contributions from the cross terms of EDV-EQ and EQ-EDV. These are not contained in the above SOA results of EDV-EQ and EQ-EDV transfer, and are represented by the coherence terms of $|e^{\mp i\mathbf{q}\cdot\mathbf{R}} + 1|^2$ in Eq. (73). This shows that in the spectral overlap approach the coherence terms $2 \cos(\mathbf{q}\cdot\mathbf{R})$ are ignored in the following approximation:

$$|e^{\mp i\mathbf{q}\cdot\mathbf{R}} + 1|^2 = 2(1 + \cos \mathbf{q}\cdot\mathbf{R}) \cong 2, \quad (80)$$

so that this approximation underestimates the energy transfer rate W by about a factor of 2 for the case of $\mathbf{q}\cdot\mathbf{R} \ll 1$. A similar consideration may apply to (EDV \leftrightarrow ED) nondiagonal energy transfer between a donor and acceptor located in a noncentrosymmetric crystal field. Therefore, besides the absence of the average over continuously varied orientations of \mathbf{R} (as it should be in a one- or two-dimensional system, or for one- or two-dimensional directional energy transfer), the t -matrix approach has additional contributions from the above cross terms if the phonon coupling occurs both at the donor and acceptor positions. However, even these additional terms are much too small to solve the discrepancy between the results from a spectral overlap calculation and experiment.³⁻⁵

VIII. CONCLUSIONS

A theoretical framework and the method of application of phonon-assisted energy transfer between rare-earth ions of the f^N electronic configuration in crystals has been presented in this study. We have focused upon diagonal and nondiagonal single-phonon-assisted processes and have emphasized the differences that occur.

First, following the HLO theory, in which the Debye model of a phonon is used, we have shown that for a nondiagonal one-phonon-assisted energy transfer process, the coherent cancellations, such as those occurring in the diagonal process, are not present. Thereby, we have formulated and discussed the transition element and transition rate for the nondiagonal process, compared the related results with the ones of the diagonal process, and pointed out the effect of an acoustic phonon with small \mathbf{q} to the nondiagonal process,

especially the $(\Delta E_{12})^2$ dependence of the energy transfer rate.

Second, the running lattice waves $Q_{\mathbf{q}}^s$ have been taken to describe phonons involved in the energy transfer process, and this takes into account the anisotropic properties and crystal structure on the atomic scale. This phonon model is even different from the one-site standing-wave model used by Satten and co-workers to account for features in vibronic sidebands, where a standing wave is a linear combination of running lattice waves. Since the f^N electron-phonon coupling has been considered to be localized, the local symmetric displacement coordinates $Q^{n\beta}$ of the shells of atoms have been taken, shell by shell, to calculate the electron-phonon coupling energy. Thereby, mechanisms have been formulated, in which we find that the difference between the coherence effects of the diagonal and nondiagonal processes is still present, just as our above observation based upon the Debye treatment of phonons. However, since the dispersion relation $\omega_s(\mathbf{q})$ is not of the Debye type, the contributions from flat parts of the phonon dispersion curves (i.e., from lattice waves with high-symmetry \mathbf{q}) are emphasized, especially that one optical phonon (even with $\mathbf{q}=0$) makes an important contribution to nondiagonal processes. This contrasts with the conclusions of HLO theory. We have also included brief discussions about the simplification of the application method of the theory, the selection rules, and coherence effects. In addition, the relationship between the widely used spectral overlap model and the t -matrix approach for nondiagonal phonon-assisted energy transfer has been examined.

Finally, we provide a brief comment upon the relative importance of various one-phonon-assisted processes, in a general sense. For centrosymmetric systems, the HLO theory is only applicable to the diagonal second-order (EQ \leftrightarrow EQ, V) processes, and not to the nondiagonal second-order (EQ \leftrightarrow EDV) processes, while the (ED \leftrightarrow EDV) processes are forbidden. Indeed, in some studies, the distinction has not been clarified between the diagonal and nondiagonal processes.⁴

If there is no inversion center, the diagonal (ED \leftrightarrow EQ, V) energy transfer process is about 10 times slower than the diagonal (ED \leftrightarrow ED, V) process, from the following argument. Using W and P to represent the energy transfer rate and single-center transition oscillator strength, respectively, Dexter¹ has given the following relation:

$$\frac{W_{DD}}{W_{DQ}} \approx \frac{P_D}{P_Q} \left(\frac{R}{\lambda} \right)^2, \quad (81)$$

where R is the donor-acceptor distance, and λ is the radiation wavelength. For rare-earth ions at noncentrosymmetric sites of crystals, typically^{21,22} $P_D/P_Q \sim 10^7$ and $(R/\lambda)^2 \sim 10^{-6}$, so that $W_{DD}/W_{DQ} \sim 10$. However, the nondiagonal (ED \leftrightarrow EDV) process is also important, since^{16,21-23} $P_{DV}/P_D \sim 10^{-8}/10^{-6} \sim 10^{-2}$, but diagonal (ED \leftrightarrow ED, V) energy transfer is already a one-order-higher process than the nondiagonal (ED \leftrightarrow EDV) process. Therefore our theory and results also make sense to rare-earth ions at noncentrosymmetric sites of crystals.

In this study we have developed a framework for the study of one-phonon-assisted energy transfer processes between rare-earth ions in solids which is significantly different from previous models. The same arguments can be followed to extend the model to two-phonon-assisted nondiagonal, i.e., (EDV \leftrightarrow EDV), or to one-phonon-assisted nondiagonal (EDV \leftrightarrow MD) energy transfer processes, and since this extension is straightforward, we do not present the results. We are now considering the application of our results to a model experimental system.

ACKNOWLEDGMENTS

This work was supported by Hong Kong UGC Research Grant CityU No. 1067/99P (to P.A.T.), National Natural Science Foundation of China Research Grant No. 10074061, and Ph.D. Training Base Fund of China Grant No. 20010358016 (to S.X.).

APPENDIX A: ELECTRON-PHONON COUPLING WITHIN THE DEBYE MODEL

The HLO model of diagonal energy transfer utilized the Debye phonon model under the isotropic approximation. Here we follow this model and provide some derivations to present the detailed expressions of the relevant electron-phonon coupling parameters. We understand that the HLO model considers a crystal to be a continuous isotropic medium, so that the details of its structure on the atomic scale and of the anisotropy are ignored.

Under the Debye phonon model, the displacement of ion j from its equilibrium position \mathbf{R}_j can be written as

$$\mathbf{u}(\mathbf{R}_j) = \sum_{s,\mathbf{q}} \frac{1}{\sqrt{NM}} Q_{\mathbf{q}}^s \mathbf{e}_{\mathbf{q}}^s e^{-i\mathbf{q}\cdot\mathbf{R}_j} \quad (\text{A1})$$

where N and M are the number of lattice sites and mass of the ion, respectively; $\mathbf{e}_{\mathbf{q}}^s$ is the real polarization unit vector of the phonon mode s , \mathbf{q} , which only depends upon the direction of the phonon wave vector \mathbf{q} and the three different types of polarization index s (corresponding to one longitudinal and two transverse modes). $Q_{\mathbf{q}}^s$ is the corresponding normal coordinate. Since \mathbf{u} is real, we have the relations

$$Q_{-\mathbf{q}}^s = Q_{\mathbf{q}}^{s*}, \quad (\text{A2})$$

if we choose

$$\mathbf{e}_{-\mathbf{q}}^s = \mathbf{e}_{\mathbf{q}}^s = \mathbf{e}_{\mathbf{q}}^{s*}. \quad (\text{A3})$$

We define the strain tensor

$$\varepsilon_{\alpha\beta}(\mathbf{R}) = \frac{\partial u_{\alpha}(\mathbf{R})}{\partial R_{\beta}} = \sum_{s,\mathbf{q}} \frac{1}{\sqrt{NM}} Q_{\mathbf{q}}^s e_{\alpha}^s(-i\mathbf{q}_{\beta}) e^{-i\mathbf{q}\cdot\mathbf{R}}, \quad (\text{A4})$$

where $\alpha, \beta = x, y, z$, and we omit the dependence upon the direction of \mathbf{q} by writing

$$e_{\alpha}^s = (\mathbf{e}_{\mathbf{q}}^s)_{\alpha}. \quad (\text{A5})$$

Based upon the isotropic properties, we have

$$\varepsilon_{\alpha\beta}(\mathbf{R}) = \frac{1}{2} [\varepsilon_{\alpha\beta}(\mathbf{R}) + \varepsilon_{\beta\alpha}(\mathbf{R})]. \quad (\text{A6})$$

We also express $Q_{\mathbf{q}}^s$ in phonon-number representation:

$$Q_{\mathbf{q}}^s = \sqrt{\frac{\hbar}{2\omega_{s,\mathbf{q}}}} (a_{\mathbf{q}}^{s+} + a_{-\mathbf{q}}^s), \quad (\text{A7})$$

where the creation operator $a_{\mathbf{q}}^{s+}$ is for \mathbf{q} , while the destruction operator $a_{-\mathbf{q}}^s$ is for $-\mathbf{q}$, to meet the requirement of Eq. (A2). Then, by combining Eqs. (A4)–(A7), we obtain

$$\varepsilon_{\alpha\beta}(\mathbf{R}) = \sum_{s,\mathbf{q}} \sqrt{\frac{\hbar}{2NM\omega_{s,\mathbf{q}}}} (a_{\mathbf{q}}^{s+} + a_{-\mathbf{q}}^s) \times \frac{(-i)}{2} (e_{\alpha}^s q_{\beta} + e_{\beta}^s q_{\alpha}) e^{-i\mathbf{q}\cdot\mathbf{R}}, \quad (\text{A8})$$

which is almost the same as formula (2.5) of Ref. 2, except (i) for the factor $(-i)$, which makes the quantity $[(i)/2](e_{\alpha}^s q_{\beta} + e_{\beta}^s q_{\alpha})$ for a certain \mathbf{q} to be the complex conjugate of that for $(-\mathbf{q})$, to guarantee that $\varepsilon_{\alpha\beta}(\mathbf{R})$ is real, and (ii) the phase factor $e^{-i\mathbf{q}\cdot\mathbf{R}}$, which occurs in Eq. (2.4) of Ref. 2.

Now we introduce the localized electron-phonon coupling Hamiltonian $H_{\text{ph}}(j)$ within this model:

$$H_{\text{ph}}(j) = \sum_{\alpha\beta} \frac{\partial H_{\text{cf}}(\mathbf{R}_j)}{\partial \varepsilon_{\alpha\beta}(\mathbf{R}_j)} \varepsilon_{\alpha\beta}(\mathbf{R}_j), \quad (\text{A9})$$

where $H_{\text{cf}}(\mathbf{R}_j)$ is the crystal field energy operator for rare-earth ion j .

Following HLO,² we approximate the tensor $\varepsilon_{\alpha\beta}$ by its average value ε over the solid angle Ω :

$$\left\langle \left| \frac{(-i)}{2} (e_{\alpha}^s q_{\beta} + e_{\beta}^s q_{\alpha}) \right|^2 \right\rangle_{\Omega} = \alpha_s q^2, \quad (\text{A10})$$

where α_s is a quantity of order of magnitude 1. Then Eq. (A9) becomes Eq. (10), while the averaged strain is given by

$$\varepsilon(\mathbf{R}_j) = \sum_{s,\mathbf{q}} \sqrt{\frac{\hbar \alpha_s q^2}{2NM\omega_{s,\mathbf{q}}}} (a_{\mathbf{q}}^{s+} + a_{-\mathbf{q}}^s) e^{-i\mathbf{q}\cdot\mathbf{R}_j}. \quad (\text{A11})$$

Thus from Eqs. (11) and (12), and utilizing the matrix element of ε from the HLO treatment,²

$$\langle n_{s,\mathbf{q}} \pm 1 | \varepsilon | n_{s,\mathbf{q}} \rangle = \sqrt{\frac{\hbar \alpha_s q^2}{2MN\omega_{s,\mathbf{q}}}} \times \left\{ \frac{\sqrt{n_{s,\mathbf{q}}+1}}{\sqrt{n_{s,\mathbf{q}}}} \right\}, \quad (\text{A12})$$

we obtain the expression (13) for $g(j)$ in Eq. (12) used in the HLO theory and similarly Eq. (14) for $f(j)$.

Furthermore, we write the crystal field energy operator as follows:

$$H_{\text{cf}}(\mathbf{R}_j) = \sum_{k,q} A_k^q(\mathbf{R}_j) D_q^k[\mathbf{r}(j)], \quad k=2,4,6, \quad (\text{A13})$$

where q is the index of a component of the k th-rank tensor D_q^k ; $A_k^q(\mathbf{R}_j)$ are the crystal field parameters of the rare-earth ion j , and the electronic operator is given by

$$D_q^k[\mathbf{r}(j)] = \sum_i r_i^k c_q^k(i) = \sqrt{\frac{4\pi}{2k+1}} \sum_i r_i^k Y_q^k(\theta_i, \varphi_i), \quad (\text{A14})$$

in which the summation i goes over all f electrons of the rare-earth ion j , so that $D_q^k[\mathbf{r}(j)]$ is the quadrupole operator, etc. Then we are able to write more detailed expressions for $H_{\text{ph}}(j)$, $g(j)$, etc.:

$$H_{\text{ph}}(j) = \sum_{k,q} \frac{\partial A_k^q(\mathbf{R}_j)}{\partial \varepsilon(\mathbf{R}_j)} \varepsilon(\mathbf{R}_j) D_q^k[\mathbf{r}(j)], \quad (\text{A15})$$

$$g(j) = \sum_{k,q} \frac{\partial A_k^q(\mathbf{R}_j)}{\partial \varepsilon(\mathbf{R}_j)} \langle j^* | D_q^k[\mathbf{r}(j)] | j^* \rangle, \quad (\text{A16})$$

$$f(j) = \sum_{k,q} \frac{\partial A_k^q(\mathbf{R}_j)}{\partial \varepsilon(\mathbf{R}_j)} \langle j | D_q^k[\mathbf{r}(j)] | j \rangle, \quad (\text{A17})$$

where

$$\frac{\partial A_k^q(\mathbf{R}_j)}{\partial \varepsilon(\mathbf{R}_j)} = \left[\sum_{\alpha\beta} \frac{\partial A_k^q(\mathbf{R}_j)}{\partial \varepsilon_{\alpha\beta}(\mathbf{R}_j)} \varepsilon_{\alpha\beta}(\mathbf{R}_j) \right] \frac{1}{\varepsilon(\mathbf{R}_j)} \quad (\text{A18})$$

is a derivative averaged over solid angles.

Now it is possible to write the coupling parameters in Eqs. (6) and (8) for the nondiagonal (EQ \leftrightarrow EDV) energy transfer process as follows:

$$g_{1_x,1^*} = \sum_{t,p} \left[\frac{\partial A_t^p(\mathbf{R}_1)}{\partial \varepsilon(\mathbf{R}_1)} \right] \langle 1_x | D_p^t[\mathbf{r}(1)] | 1^* \rangle, \quad (\text{A19})$$

$$f_{2_x,2} = \sum_{t,p} \left[\frac{\partial A_t^p(\mathbf{R}_2)}{\partial \varepsilon(\mathbf{R}_2)} \right] \langle 2_x | D_p^t[\mathbf{r}(2)] | 2 \rangle, \quad (\text{A20})$$

and so on, where $t=1, 3, 5, 7$ are odd numbers and $D_p^1[\mathbf{r}(1)]$ is the dipole operator of ion 1, etc., since the parity of the virtual intermediate states $|1_x\rangle$ or $|2_x\rangle$ is opposite to that of the f^N -electron states $|1^*\rangle$ or $|2\rangle$, etc. The coupling coefficients, like in Eq. (A18), are key factors for estimating the values of the g 's and f 's coupling parameters in Eqs. (A16), (A17), (A19) and (A20).

APPENDIX B: THE SHELL MODEL AND THE LATTICE WAVE MODEL OF PHONONS AND THEIR RELATIONSHIP

1. For the shell model, the transformation matrix $a_\alpha^{n\beta}(\mathbf{d}_n)$ in Eq. (44) is orthogonal (real unitary):

$$\sum_\beta a_\alpha^{n\beta}(\mathbf{d}_n)^* a_{\alpha'}^{n\beta}(\mathbf{d}'_n) = \sum_\beta a_\alpha^{n\beta}(\mathbf{d}_n) a_{\alpha'}^{n\beta}(\mathbf{d}'_n) = \delta_{\mathbf{d}_n \mathbf{d}'_n} \delta_{\alpha\alpha'}. \quad (\text{B1})$$

and

$$\sum_{\mathbf{d}_n, \alpha} a_\alpha^{n\beta}(\mathbf{d}_n)^* a_\alpha^{n\beta'}(\mathbf{d}_n) = \sum_{\mathbf{d}_n, \alpha} a_\alpha^{n\beta}(\mathbf{d}_n) a_\alpha^{n\beta'}(\mathbf{d}_n) = \delta_{\beta\beta'}, \quad (\text{B2})$$

so we obtain from them and Eq. (44)

$$\sqrt{M_n} u_\alpha(\mathbf{d}_n) = \sum_\beta a_\alpha^{n\beta}(\mathbf{d}_n) Q^{n\beta}(D). \quad (\text{B3})$$

2. The normal coordinates of lattice waves $Q_{\mathbf{q}}^s$ are defined in Eqs. (46) and (47). Note that when \mathbf{q} is not on the surface of the Brillouin zone, the irrep s of the space group $\mathcal{S}(\mathbf{q})$ in Eq. (47) can be represented instead by the irrep of the point group $\mathcal{P}(\mathbf{q})$ of the wave vector \mathbf{q} , which is a subgroup of the crystallographic point group \mathcal{G}_0 and is isomorphic to the factor group $\mathcal{S}(\mathbf{q})/\mathcal{T}(\mathbf{I})$ of the space group $\mathcal{S}(\mathbf{q})$, with respect to its translation subgroup $\mathcal{T}(\mathbf{I})$.

The transformation matrix in Eq. (46) is complex unitary:

$$\sum_s a_\alpha^{\mathbf{q}s}(\mathbf{p})^* a_\alpha^{\mathbf{q}s}(\mathbf{p}') = \delta_{\alpha\alpha'} \delta_{\mathbf{p}\mathbf{p}'}, \quad (\text{B4})$$

$$\sum_{\alpha\mathbf{p}} a_\alpha^{\mathbf{q}s}(\mathbf{p})^* a_\alpha^{\mathbf{q}s'}(\mathbf{p}) = \delta_{s s'}. \quad (\text{B5})$$

From Eqs. (46) and (B4) and noticing $\sum_{\mathbf{q}} e^{-i\mathbf{q}\cdot(\mathbf{R}_l - \mathbf{R}_m)} = N \delta_{\mathbf{R}_l, \mathbf{R}_m}$, we obtain Eq. (48).

3. We now observe that a certain atom can be identified by $(\mathbf{R}_1 + \mathbf{d}_n)$ or $(\mathbf{R}_2 + \mathbf{a}_n)$, and also by $(\mathbf{R}_l + \mathbf{p})$. It is not difficult to establish the following relations:

$$\mathbf{R}_l = \mathbf{R}_l(\mathbf{d}_n) \text{ or } \mathbf{R}_l(\mathbf{a}_n), \quad (\text{B6})$$

$$\mathbf{p} = \mathbf{p}(\mathbf{d}_n) \text{ or } \mathbf{p}(\mathbf{a}_n). \quad (\text{B7})$$

Substituting Eq. (48) and Eqs. (B6) and (B7) into Eq. (44) we obtain

$$\begin{aligned} Q^{n\beta} &= \sum_{\mathbf{d}_n, \alpha} a_\alpha^{n\beta}(\mathbf{d}_n)^* \sqrt{M_p} u_\alpha[\mathbf{R}_l(\mathbf{d}_n), \mathbf{p}(\mathbf{d}_n)], \\ &= \frac{1}{\sqrt{N}} \sum_{\mathbf{d}_n, \alpha} a_\alpha^{n\beta}(\mathbf{d}_n)^* a_\alpha^{\mathbf{q}s}[\mathbf{p}(\mathbf{d}_n)] e^{i\mathbf{q}\cdot\mathbf{R}_l(\mathbf{d}_n)} Q_{\mathbf{q}}^s, \end{aligned} \quad (\text{B8})$$

and therefore obtain Eq. (49).

**APPENDIX C: ELECTRON-PHONON COUPLING
WITHIN THE SHELL MODEL
AND THE LATTICE WAVE MODEL**

1. The localized electron-phonon coupling Hamiltonian $H_{\text{ph}}(1)$ is expanded in Eq. (54) by means of the shell model, in which the expansion coefficients $f_{n\beta}(D)$ can be written as

$$f_{n\beta}(D) = \frac{\partial H_{\text{cf}}(\mathbf{R}_1)}{\partial Q^{n\beta}(D)} = \sum_{t,p} \frac{\partial A_p^t(D)}{\partial Q^{n\beta}(D)} D_p^t(D). \quad (\text{C1})$$

In the second step of Eq. (C1), $H_{\text{cf}}(\mathbf{R}_1)$ has been expressed using a crystal field model, like Eq. (A13), where $A_p^t(D)$ are crystal field parameters and $D_p^t(D)$ are electronic multipole operators of the donor ion. The index $t=1,2,3,\dots,7$; $p=t, t-1, \dots, -t$; and the shell number $n=0,1,2,\dots$.

2. It is not difficult to derive another expressions for the coupling coefficient $f_{n\beta}(D)$ as follows:

$$\begin{aligned} f_{n\beta}(D) &= \frac{\partial H_{\text{cf}}(\mathbf{R}_1)}{\partial Q^{n\beta}(D)} = \sum_{\mathbf{d}_n, \alpha} \frac{\partial H_{\text{cf}}(\mathbf{R}_1)}{\partial u_\alpha(\mathbf{d}_n)} \frac{\partial u_\alpha(\mathbf{d}_n)}{\partial Q^{n\beta}(D)} \\ &= \sum_{\mathbf{d}_n, \alpha} \frac{\partial H_{\text{cf}}(\mathbf{R}_1)}{\partial u_\alpha(\mathbf{d}_n)} \frac{a_\alpha^{n\beta}(\mathbf{d}_n)}{\sqrt{M_n}}, \end{aligned} \quad (\text{C2})$$

where Eq. (B3) has been used.

Furthermore, by substituting Eqs. (50) and (C2) into Eq. (55), and using Eq. (B1), we have

$$\begin{aligned} H_{\text{ph}}(1) &= \sum_{n\beta} \sum_{\mathbf{d}_n, \alpha} \left[\frac{\partial H_{\text{cf}}(\mathbf{R}_1)}{\partial u_\alpha(\mathbf{d}_n)} \right] \frac{a_\alpha^{n\beta}(\mathbf{d}_n)}{\sqrt{M_n}} \\ &\quad \times \sum_{\mathbf{q}, s} \sum_{\mathbf{d}'_n, \alpha'} a_{\alpha'}^{n\beta}(\mathbf{d}'_n) * a_\alpha^{\text{qs}}[\mathbf{p}(\mathbf{d}'_n)] e^{i\mathbf{q} \cdot \mathbf{R}_l(\mathbf{d}'_n)} Q_{\mathbf{q}}^s \frac{1}{\sqrt{N}} \\ &= \sum_n \sum_{\mathbf{d}_n, \alpha} \left[\frac{\partial H_{\text{cf}}(\mathbf{R}_1)}{\partial u_\alpha(\mathbf{d}_n)} \right] \frac{1}{\sqrt{NM_n}} \\ &\quad \times \sum_{\mathbf{q}, s} a_\alpha^{\text{qs}}[\mathbf{p}(\mathbf{d}_n)] e^{i\mathbf{q} \cdot \mathbf{R}_l(\mathbf{d}_n)} Q_{\mathbf{q}}^s. \end{aligned} \quad (\text{C3})$$

This equation presents a direct way to calculate the coupling energy of all lattice waves $Q_{\mathbf{q}}^s$ via the respective vibrations of all shell atoms \mathbf{d}_n participating in the movements of these lattice waves (we still can ignore all shell atoms with $n > n_{\text{max}}$). Note that the local site-symmetry displacements $Q^{n\beta}$ are omitted so that the irrep symbol β of group \mathcal{G} thereby disappears. However, if we use the electronic operator $f_{n\beta}(D)$ instead of $[\partial H_{\text{cf}}(\mathbf{R}_1)/\partial u_\alpha(\mathbf{d}_n)]$, it is easier to discuss the selection rule of the pertinent electronic transition, since the electronic states are bases of the irrep $[\beta$ in Eq. (45)] of the rare-earth site symmetry point group \mathcal{G} .

3. In order to calculate the electronic operator $[\partial H_{\text{cf}}(\mathbf{R}_1)/\partial u_\alpha(\mathbf{d}_n)]$ in Eqs. (C3) and (C2), we may expand the crystal field energy $H_{\text{cf}}(\mathbf{R}_1)$ of the donor as a sum of the interaction energies $V(\mathbf{d}_n)$ between each shell atom \mathbf{d}_n ($n \neq 0$) and the f^N electrons of the donor ion \mathbf{d}_0 :

$$H_{\text{cf}}(\mathbf{R}_1) = \sum_n' V(\mathbf{d}_n), \quad (\text{C4})$$

where Σ' means that $V(\mathbf{d}_0)$ is not included. Therefore, we have

$$\frac{\partial H_{\text{cf}}(\mathbf{R}_1)}{\partial u_\alpha(\mathbf{d}_n)} = \frac{\partial V(\mathbf{d}_n)}{\partial u_\alpha(\mathbf{d}_n)}, \quad (\text{C5})$$

which permits the calculation of the $f_{n\beta}(D)$ in Eqs. (C2) and (55), and of the $H_{\text{ph}}(1)$ in Eq. (C3).

Furthermore, based on Eq. (C5), we may make Eq. (C3) more simple. Notice that $V(\mathbf{d}_n)$ is the interaction energy between atom \mathbf{d}_n and rare-earth ion \mathbf{d}_0 , so that¹¹

$$\frac{\partial V(\mathbf{d}_n)}{\partial u_\alpha(\mathbf{d}_0)} = - \frac{\partial V(\mathbf{d}_n)}{\partial u_\alpha(\mathbf{d}_n)}. \quad (\text{C6})$$

Thus we can write the terms with $n=0$ in Eq. (54), by referring to Eqs. (C2), (44), (B1), and (C4):

$$\begin{aligned} &\sum_\beta f_{0\beta}(D) Q^{0\beta}(D) \\ &= \sum_\beta \left[\sum_\alpha \frac{\partial H_{\text{cf}}(\mathbf{R}_1)}{\partial u_\alpha(\mathbf{d}_0)} \frac{a_\alpha^{0\beta}(\mathbf{d}_0)}{\sqrt{M_0}} \right] \left[\sum_{\alpha'} a_{\alpha'}^{0\beta}(\mathbf{d}_0) * \sqrt{M_0} u_{\alpha'}(\mathbf{d}_0) \right] \\ &= \sum_\alpha \frac{\partial H_{\text{cf}}(\mathbf{R}_1)}{\partial u_\alpha(\mathbf{d}_0)} u_\alpha(\mathbf{d}_0) \\ &= \sum_\alpha \left[\sum_n' \frac{\partial V(\mathbf{d}_n)}{\partial u_\alpha(\mathbf{d}_0)} \right] u_\alpha(\mathbf{d}_0) \\ &= \sum_\alpha \sum_n' \frac{\partial V(\mathbf{d}_n)}{\partial u_\alpha(\mathbf{d}_n)} [-u_\alpha(\mathbf{d}_0)]. \end{aligned} \quad (\text{C7})$$

Similarly

$$\sum_{n(\geq 1)} \sum_\beta f_{n\beta}(D) Q^{n\beta}(D) = \sum_{n(\geq 1)} \sum_{\mathbf{d}_n, \alpha} \frac{\partial V(\mathbf{d}_n)}{\partial u_\alpha(\mathbf{d}_n)} u_\alpha(\mathbf{d}_n), \quad (\text{C8})$$

so that Eq. (54) becomes

$$\begin{aligned} H_{\text{ph}}(1) &= \sum_{\alpha\beta} f_{n\beta}(D) Q^{n\beta}(D) \\ &= \sum_{n(\geq 1)} \sum_{\mathbf{d}_n, \alpha} \frac{\partial V(\mathbf{d}_n)}{\partial u_\alpha(\mathbf{d}_n)} [u_\alpha(\mathbf{d}_n) - u_\alpha(\mathbf{d}_0)], \end{aligned} \quad (\text{C9})$$

which is decided by the relative displacement $[u_\alpha(\mathbf{d}_n) - u_\alpha(\mathbf{d}_0)]$, as it should be. Equation (C9) provides a direct way to calculate $H_{\text{ph}}(1)$ from atomic displacements.

- ¹D. L. Dexter, *J. Chem. Phys.* **21**, 836 (1953).
- ²T. Holstein, S. K. Lyo, and R. Orbach, in *Topics in Applied Physics*, edited by W. M. Yen and P. M. Selzer (Springer-Verlag, New York, 1981), Vol. 49, Chap. 2; and R. Orbach, in *Optical Properties of Ions in Crystals*, edited by H. M. Crosswhite and H. W. Moos (Interscience, New York, 1967), p. 445.
- ³M. Chua, P. A. Tanner, and M. F. Reid, *J. Lumin.* **60&61**, 838 (1994).
- ⁴D. M. Moran, P. S. May, and F. S. Richardson, *Chem. Phys.* **186**, 77 (1994).
- ⁵P. A. Tanner, M. Chua, and M. F. Reid, *J. Alloys Compd.* **225**, 20 (1995).
- ⁶W. E. Bron, *Phys. Rev.* **140**, A2005 (1965).
- ⁷T. Kushida, *J. Phys. Soc. Jpn.* **34**, 1318 (1973).
- ⁸T. R. Faulkner and F. S. Richardson, *Mol. Phys.* **35**, 1141 (1978).
- ⁹B. R. Judd, *Phys. Rev.* **127**, 181 (1962).
- ¹⁰S. L. Chodos and R. A. Satten, *J. Chem. Phys.* **62**, 2411 (1975).
- ¹¹E. Cohen and H. W. Moos, *Phys. Rev.* **161**, 258 (1967).
- ¹²I. Richman, R. A. Satten, and E. Y. Wong, *J. Chem. Phys.* **39**, 1833 (1963).
- ¹³R. A. Satten, *J. Chem. Phys.* **40**, 1200 (1964).
- ¹⁴E. Cohen and H. W. Moos, *Phys. Rev.* **161**, 268 (1967).
- ¹⁵P. Morley, T. R. Faulkner, and F. S. Richardson, *J. Chem. Phys.* **77**, 1710 (1982).
- ¹⁶B. R. Judd, *Phys. Scr.* **21**, 543 (1980).
- ¹⁷S. M. Crooks, M. F. Reid, P. A. Tanner, and Y. Y. Zhao, *J. Alloys Compd.* **250**, 297 (1997).
- ¹⁸S. L. Chodos, *J. Chem. Phys.* **57**, 2712 (1972).
- ¹⁹G. P. O'Leary and R. G. Wheeler, *Phys. Rev. B* **1**, 4409 (1970).
- ²⁰R. S. Sinkovits and R. H. Bartram, *J. Phys. Chem. Solids* **52**, 1137 (1991).
- ²¹S. Hubert, D. Meichenin, B. W. Zhou, and F. Auzel, *J. Lumin.* **50**, 7 (1991).
- ²²P. A. Tanner and G. G. Siu, *Mol. Phys.* **75**, 233 (1992).
- ²³R. Acevedo, P. A. Tanner, T. Meruane, and V. Poblete, *Phys. Rev. B* **54**, 3976 (1996).